[Short title + Author Name - P&H title] 17 (2024) 105896

Contents lists available at ScienceDirect

Arabian Journal of Chemistry

journal homepage: www.ksu.edu.sa

Kinetic study of *in vitro* release of curcumin from chitosan biopolymer and the evaluation of biological efficacy

Supuni Wijayawardana, Charitha Thambiliyagodage *, Madara Jayanetti

Faculty of Humanities and Sciences, Sri Lanka Institute of Information Technology, New Kandy Road, Malabe, Colombo, Sri Lanka

ARTICLE INFO

Keywords:
Curcumin
Chitosan
Drug delivery
Anti-oxidant
Anti-inflammatory

ABSTRACT

Sustained release of curcumin from the polymeric carrier system chitosan, a natural biopolymer material derived from chitin originated from natural shrimp shell waste, was studied. Six kinetic models, zero order, first order, Korsmeyer–Peppas (KP), Peppas – Sahlin (PS), Higuchi, and Hixson–Crowell, were applied to study the drug release kinetics. The release mechanism of the drug from the curcumin-chitosan composite was evaluated by changing the pH, ionic strength of the release media, and drug concentration. KP and PS models were selected among the studied models to investigate the drug release mechanism from the chitosan biopolymer based on the R^2 values ($R^2 > 0.99$). The model constants *m* in the PS model and n in the KP model stand for the case II relaxation and Fickian diffusion contribution, respectively. The *n* being < 0.43 in the KP model suggests that the Fickian diffusion governs the drug release. Furthermore, there is a noticeable difference between the values obtained for model parameters *m* and *n* in the PS and KP models, indicating that Case II relaxation and Fickian diffusion play crucial roles in the curcumin release mechanism from chitosan. Polymer relaxation has been proven to play a predominant role in releasing curcumin from the composite at lower ionic strengths and higher pH values. Anti-inflammatory activity was tested using the egg-albumin denaturation assay, and the diphenyl-2-picrylhydrazyl assay was carried out to determine the antioxidant activity of the composite. The composite material showed IC_{50} values of 0.29 mg/ mL and 1.08 mg/ mL for anti-inflammatory and anti-oxidant activities, respectively. The drug composite has shown antibacterial activity against *Pseudomonas aeruginosa*, *Klebsiella pneumoniae*, and *Staphylococcus aureus*, which are highly effective against *S.aureus*. The resulting inhibition zones for *S.aureus* were 13.34 ± 0.34 mm, 16.34 ± 0.60 mm, and 13.34 ± 0.73 mm for 5, 10, and 20 mg/ml concentrations, respectively. The drug composite's minimum inhibitory concentration/ minimum bactericidal concentration ratio for *S.aureus, K. pneumoniae,* and *P.aeruginosa* was greater than 4, suggesting that they cause bacteriostatic effects.

1. Introduction

Turmeric, scientifically known as *Curcuma longa* L., is derived from a rhizomatous herbaceous perennial flowering plant belonging to the ginger family (Zingiberaceae) (Bagheri et al., 2020). It contains four main types of curcuminoids: curcumin, demethoxycurcumin, bisdemethoxycurcumin, and cyclocurcumin (Hu & Luo, 2021; Huang & Beevers, 2011). Chemically, curcumin is a diarylheptanoid identified as 1,7-bis (4-hydroxy-3-methoxyphenyl)-1,6-heptadien-3,5-dione with two aromatic O-methoxy phenolic groups, which are connected by two α, β-unsaturated carbonyl groups (Hu & Luo, 2021; Yixuan et al., 2021). The enol form of the carbon-4 of the heptane linker functions mainly as an electron donor, and it can also be a substantial proton donor in its bis-keto form (Huang & Beevers, 2011). Due to the above-described chemical characteristics of the molecule (Huang & Beevers, 2011), it exhibits limited solubility in water while it readily dissolves in organic solvents like dimethyl sulfoxide, ethanol, methanol, or acetone (Perrone et al., 2015; Yixuan et al., 2021). The antioxidant properties of curcumin are higher than those of ascorbic acid (Naksuriya & Okonogi, 2015). In addition to the antioxidant properties, curcumin possesses antibacterial (Gunes et al., 2016; Zheng et al., 2020), anti-tumor (Abadi et al., 2022; Khar et al., 1999; Santel et al., 2008), and chemosensitizing (Kwon, 2014) properties, as well as they are capable of modifying the lipid profile (Panahi et al., 2017) and offer protection to the liver (Farzaei et al., 2018), blood vessels, heart (Jiang et al., 2017; Wongcharoen & Phrommintikul, 2009), lungs (Venkatesan et al., 2007), and nerves

* Corresponding author.
E-mail address: charitha.t@sliit.lk (C. Thambiliyagodage).

https://doi.org/10.1016/j.arabjc.2024.105896
Received 15 April 2024; Accepted 3 July 2024
Available online 6 July 2024

(Kulkarni & Dhir, 2010). Moreover, curcumin also exhibits antithrombotic (Keihanian et al., 2018), immunomodulatory (Srivastava et al., 2011), antidiabetic (Den Hartogh et al., 2019, 2020), anti-inflammatory (Y. Peng et al., 2021), particularly anti-neuroinflammatory, and microglia-activation inhibitory effects (Cianciulli et al., 2022; Yu et al., 2018), due to which it has become the focus of attention in recent research, particularly related to Alzheimer's condition (Ahmed & Gilani, 2014; Bagheri et al., 2020; Hamaguchi et al., 2010a; Mishra & Palanivelu, 2008; Wechsler et al., 2019).

It is commonly known that curcumin exhibits a low pharmacokinetic profile, poor water solubility, and chemical instability (Anand et al., 2007; Cas & Ghidoni, 2019; W. Liu et al., 2016; Mirzaei et al., 2017). Even when consumed at larger dosages (12 g/day), curcumin's bioavailability in humans is relatively low, raising questions about its therapeutic potential despite its efficacy and safety (Mantzorou et al., 2018). Research conducted thus far on the pharmacokinetics of curcumin has demonstrated that the drug's fast metabolism (Metzler et al., 2013) and poor absorption significantly reduce its bioavailability due to its small intestine's low absorption (Anand et al., 2007; Metzler et al., 2013), the liver's significant reductive and conjugative metabolism (Pandey et al., 2017), and the gall bladder's removal of the substance (W. Liu et al., 2016). Hence, novel drug delivery systems should be developed to improve the biocompatibility of curcumin and enhance drug delivery in biological systems. In recent studies, strategies such as liposome, nanoparticles such as poly butylcyanocrylate (PBCA) nanoparticles, poly lactide-co-glycolide (PLGA) nanoparticles, chitosan (CS) nanoparticles, polymeric micelles, nano gels, nanoemulsions, and dendrimers & dimers have been used to increase curcumin's pharmacokinetic properties.

Due to its vital biological and biomechanical characteristics as well as its distinct cationic nature, chitosan (CS) is utilized to target several potential biomedical applications including drug delivery systems (Ahmad et al., 2020; Dutta & Ikiki, 2014; Eltaweil et al., 2023; Gull et al., 2019; Mirzaei et al., 2017; Mohebbi et al., 2018; Quadrado & Fajardo, 2020; Sun et al., 2012; Varukattu et al., 2020). Chitosan biopolymer has been suggested as a potential delivery system for curcumin (Herdiana et al., 2022; Hu & Luo, 2021; Samrot et al., 2018; Thambiliyagodage et al., 2023). Chitosan is a linear copolymer polysaccharide categorized by a random arrangement of β (1 → 4) connected 2-amino-2-deoxy-D-glucose (D-glucosamine) and 2-acetamido-2-deoxy-D-glucose (N-acetyl-D-glucosamine) units (Saikia & Gogoi, 2015). It is being used in medical settings, such as sutures (Prabha et al., 2021), tissue engineering (Kim et al., 2023), gene therapy (Jayakumar et al., 2010), and implants (Shariatinia, 2019) because of its biocompatibility (Ali & Ahmed, 2018; Mohebbi et al., 2018; Thandapani et al., 2017), non-toxicity, and antibacterial (Chandrasekaran et al., 2020; Li & Zhuang, 2020; Verlee et al., 2017) qualities. In addition, chitin promotes wound healing and mucoadhesion and has the potential to be used in controlled drug release (Gouda et al., 2022; Herdiana et al., 2022; Morin-Crini et al., 2019; Thambiliyagodage et al., 2023).

Researchers still have difficulty precisely delivering pharmacologically active substances, which prompted the creation of drug delivery systems. They can provide better bioavailability, extended drug presence in the target tissue, enhanced stability for therapeutic compounds against chemical and enzymatic degradation, and precise drug targeting by including specific ligands (Saikia & Gogoi, 2015; Shariatinia, 2019). The methods available to use to regulate the release of the drug from the polymer are surface degradation of the polymer matrix, breaking of polymer bonds at the bulk matrix or on the surface, and drug diffusion (Lao et al., 2011; Unagolla & Jayasuriya, 2018). Either one of them or a combination of the above methods can release the drug molecules (Unagolla & Jayasuriya, 2018). Controlled release systems are classified into four categories based on drug release mechanisms: diffusion-controlled, chemically controlled, osmotically controlled, and swelling and dissolution-controlled (Peppas & Narasimhan, 2014). Mathematical models have been used to estimate the sustained release of the drug molecules, evaluate the drug-releasing mechanisms through the collected experimental data, and further facilitate the design of drug molecules with optimal release profiles (Peppas & Narasimhan, 2014). Such mathematical models employed to determine the kinetic analysis of drug release from chitosan are the zero-order model, first-order model, Higuchi model, Hixson-Crowell (HC), Peppas-Sahlin (PS) and Korsmeyer and Peppas (KP) model (Marcos et al., 2015; Peppas & Narasimhan, 2014). Diffusion-controlled systems, which can be explained using models like zero order, first order, Higuchi, and Korsmeyer and Peppas, utilize a sequestered polymer membrane with a core containing a bioactive cargo molecule (Peppas & Narasimhan, 2014). This method is generally applied to hydrophilic drug molecules. Hydrophobic drug molecules tend to be released through swelling (dissolution) or erosion of the polymer matrix (Marcos et al., 2015).

Even though curcumin has attracted interest due to its pharmacological importance, its lower bioavailability cannot be used as a direct drug through oral or intravenous administration routes.

Though *in vitro* studies on release of curcumin bound to chitosan nanoparticles have been studied by Ali & Ahmed (Ali & Ahmed, 2018); Barbara et al. (Barbara et al., 2017); Herdiana et al. (Herdiana et al., 2022); Hu & Luo (Hu & Luo, 2021); Saikia & Gogoi (Saikia & Gogoi, 2015); Sun et al. (Sun et al., 2012) bind of curcumin to chitosan biopolymer extracted from natural waste shrimp shells and release of curcumin according to the above-mentioned mathematical models have not been reported to our knowledge. Further, curcumin-bound chitosan's antibacterial activity on gram-negative and positive bacteria has not been studied before. Here, we report the kinetic models of releasing curcumin from chitosan biopolymer and the *in vitro* influence of the composites on the growth of the test organisms *Staphylococcus aureus*, *Escherichia coli*, *Klebsiella pneumoniae* and *Pseudomonas aeruginosa*.

2. Methodology

2.1. Extraction of curcumin from turmeric rhizome

Curcuma longa L (turmeric) rhizomes were collected, washed, and peeled to remove any impurities on the outer surface. They were cut into thin pieces and oven-dried at 45 °C overnight. Then, they were ground using a mechanical grinder to obtain the turmeric powder. Turmeric powder (10 g) was subjected to double organic extraction using 100 mL of 80 % ethanol as the solvent following the heated sonication (45 °C for 3 h) to obtain the curcumin extract. Soner 203H Heated Ultrasonic Cleaner, 35 KHz, was used for the extraction process. The crude extract of curcumin was obtained after successful evaporation of ethanol.

2.2. Synthesis of chitosan from waste shrimp shells

Waste shrimp shells of shrimp varieties *Penaeus monodon* and *Penaeus vannamei* were collected and cleaned by removing the pleopods and pereiopods. The resulting shrimp shells were washed several times with tap water and distilled water, followed by washing with 70 % isopropyl alcohol to remove impurities adhered to the shells. Cleaned shells were then oven-dried at 80 °C for 3 h and ground using a grinder until a fine powder resulted. Demineralization, which is the removal of $CaCO_3$ and $Ca_3(PO_4)_2$, was carried out using 10 % (v/v) HCl solution for 24 h under constant stirring. The samples were washed with distilled water to obtain a neutral pH. The resulting powder was then suspended in a 3 % (w/v) NaOH solution for 5 h under constant stirring for the deproteination step. Deacetylation was conducted by reflux condensation (2 h at 80 °C) using a 50 % (w/v) solution of NaOH. Through this step, chitin present in the shrimp shell was converted to higher molecular weight chitosan, and the resulting powder was washed using distilled water until a neutral pH was obtained. Chitosan was oven-dried overnight at 80 °C and stored in a reagent bottle for future usage and analysis (Mendis et al., 2023).

2.3. Synthesis of the curcumin-chitosan composite material

Chitosan (1 g) powder was dispersed in the ethanolic extract of curcumin (0.1 g/ml) and allowed for casting, absorbing, and grafting of curcumin to the chitosan biopolymer under slow constant stirring at 100 rpm for three days at room temperature. Then, the resulting composite material (chitosan: curcumin, 1:10) was oven-dried at 40 °C to remove any moisture retained and stored in an airtight container for future use and analysis. The total synthesis procedure of the curcumin chitosan composite is illustrated in Scheme 1.

2.4. Characterization of synthesized materials

The Rigaku Ultima IV system, which uses Cu Kα (λ = 0.154 nm) radiation varying the 2θ from 10 ° to 80 ° at a scan speed of 2 °/min, was utilized to obtain crystallographic structure patterns of turmeric powder, chitosan, and the synthesized composite material. The surface morphology of the synthesized chitosan and composite was evaluated using ZEISS EVO 18 RESEARCH field-emission SEM.

2.5. Anti-inflammatory activity – Egg albumin denaturation assay

The *in vitro* anti-inflammatory activity of the curcumin extract and drug composite was assessed according to Yesmin et al.(Yesmin et al., 2020) Banerjee et al.(Banerjee et al., 2014) with slight modifications. The reaction mixture (5 mL) consisted of 0.2 ml of 1 % (w/v) egg albumin with 2.8 mL phosphate buffer saline (PBS, pH 6.4) and 2 mL of changing concentrations (100 µg/mL – 1600 µg/mL) of curcumin extract and composite material in methanol. A mixture of 0.2 mL of 1 % egg albumin, 2 mL methanol (without the plant extract), and 2.8 mL of PBS was used as the control substance. Samples were incubated at 37 °C for 30 min and heated in a water bath for 15 min at 70 °C. After that, absorbance was measured at 660 nm, and the experiment was triplicated. The following formula (1) was used for calculating the percentage inhibition of protein denaturation: (Banerjee et al., 2014)

$$\%\ \text{inhibition of egg albumin denaturation} = \frac{Absofsample - Absofcontrol}{Absofcontrol} \times 100 \quad (1)$$

The IC_{50} value was determined by plotting the % inhibition over-concentration on a linear model. Results were reported as mean % inhibition ± standard error. Diclofenac sodium was used as the positive control.

2.6. Antioxidant activity – diphenyl picrylhydrazyl (DPPH) assay

According to the protocol reported by Ak & Gülçin (Ak & Gülçin, 2008), utilizing a stable 1,1-diphenyl-2-picrylhydrazyl (DPPH) solution, the overall antioxidant potential of curcumin and the composite material was assessed. The 1 mg/mL stock solution of the samples was diluted with methanol to produce 5 mL of reaction mixture with the final concentrations of $5, 10, 15, 20 and 25 \mu g/mL$ for curcumin extract and $10, 20, 30, 40, 50, 60 and 70 \mu g/mL$ for the composite material. For each reaction mixture, 0.5 mL from the one mM stock DPPH solution was added. The DPPH absorbance was measured against a blank (methanol 5 mL and 0.5 mL of DPPH) after 30 min of incubation in the dark. The radical scavenging ability (RSA%) of the extract is proportional to the decline of the absorbance after adding the stable DPPH radical to the extract. This analysis was performed in triplicate (n = 3), and the results were expressed as mean % inhibition of the DPPH radical/ RSA% ± SE, which was calculated as follows (2): (Ak & Gülçin, 2008)

$$\%\ \text{inhibition}/\ \text{RSA\%} = \frac{Absofcontrol - Absofsample}{Absofcomtrol} \times 100 \quad (2)$$

The concentration of sample that could scavenge half of the DPPH radical (IC_{50}) was calculated by plotting the RSA% over-concentration on a linear model. Ascorbic acid was used as the positive control in the assay (Al-Abdallah et al., 2022a).

2.7. In vitro drug release studies

In vitro drug release of the synthesized composite material was assessed over different pH conditions varying from pH 1, 2.5, 4, 5.5, 7, 7.4, 8.5, and 10. Further, the ionic strength of the release medium was changed by varying the NaCl concentration from 0.1 M – to 0.5 M. For the analysis, 5 mg of the composite material was added to the release medium in a cuvette, and the release data was collected at 15-minute intervals for 10 h using a visible range spectrophotometer. From the absorbance values, the pH media and the NaCl concentration, which showed the best release, were selected. To determine dose-dependent release, a media with a NaCl concentration of 0.3 M and pH of 7.4 was prepared. Drug release was measured in the prepared media by changing the composite weight to 2.5 mg, 5 mg, 7.5 mg, and 10 mg.

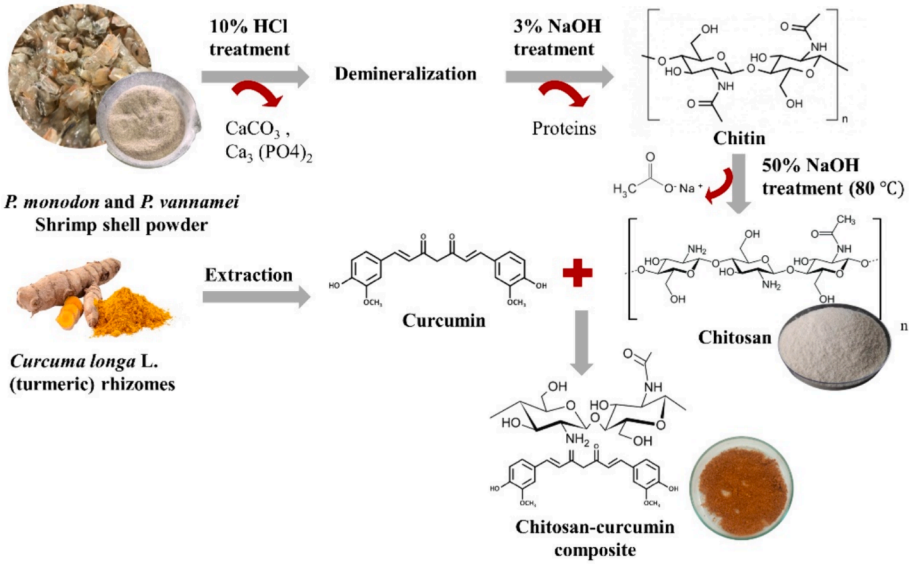

Scheme 1. Schematic representation – the synthesis of chitosan curcumin composite from the raw materials.

Drug release data was converted to the cumulative drug release % (% CDR) using the Eq. (3):

$$\%CDR = \frac{Absorbancevalueattimet_1}{Totalamountofdrugencapsulatedwithdeliverysystem} \times 100 \quad (3)$$

To determine the total amount of drug encapsulated in chitosan biopolymer, a turmeric powder-to-biopolymer ratio was used, assuming that curcumin was the main phytochemical extracted from ethanolic media in the extraction process.

2.7.1. Drug release kinetic models

To evaluate the release mechanisms of the drug composite from the chitosan biopolymer, the obtained release data at different pH values, ionic strengths, and different drug concentrations were fitted with six kinetic models: zero-order, first-order, Korsmeyer – Peppas, Peppas–Sahlin model, Higuchi model, and Hixson–Crowell models, respectively (Marcos et al., 2015).

The description of the zero-order kinetic model is provided by Eq. (4). Zero-order kinetics were used when the drug release kinetics were dependent on concentration. (Marcos Luciano Bruschi, 2015)

$$m_t = m_b k_0 t \quad (4)$$

Where m_t is the amount of drug released in time t, m_b is the initial concentration of the drug in the solution before release, and k_0 is the zero-order release rate constant.

When there is a concentration dependence in the drug release, first-order kinetics (Eq. (5)) is applied to describe the release. (Marcos Luciano Bruschi, 2015)

$$Logm_t = logm_b - \frac{k_t}{2.203} \quad (5)$$

Where m_t is the amount of the released drug in time t, m_b is the initial concentration of the drug, and K_t is the first-order rate constant.

The Korsmeyer – Peppas kinetic model is as follows (Eq. (6)): (Marcos Luciano Bruschi, 2015)

$$\log(M_t/M_\infty) = \log k_{K-P} + n\log t \quad (6)$$

Where k_{K-P} is the Korsmeyer – Peppas rate constant, n is the diffusional exponent used to characterize the drug release mechanism, and m_∞ is the amount of drug released after an infinitive time (in our case, after 600 min). The form of the drug carrier system generally affects the value of n. In spherically shaped systems where Fickian diffusion release is found, the n value is found to be 0.43. In contrast, a non-Fickian diffusion release, or anomalous transport mechanism, is suggested if $0.43 < n < 0.89$. If n is more than 0.89, the drug release is mostly governed by the case II release mechanism, which combines the processes of diffusion and swelling-controlled release (Mohan et al., 2022).

The estimated diffusional and relaxational contributing mechanisms in an anomalous drug release process were determined using the Peppas-Sahlin model (Eq. (7)) (Marcos Luciano Bruschi, 2015)

$$\frac{M_t}{M_\infty} = K_1 t^m + K_2 t^{2m} \quad (7)$$

Where the constants K_1, K_2, and m are found. When looking at the right side of the equation, the Case II relaxational contribution is represented by the second term, while the Fickian diffusional contribution (F) is represented by the first term (R). For every system with controlled release, the strictly Fickian diffusion exponent is represented by the coefficient m. The following formula (Eq. (8)) can be used to determine the ratio of the R and F contributions: (Marcos Luciano Bruschi, 2015)

$$\frac{R}{F} = \frac{K_2 t^m}{K_1} \quad (8)$$

Eq. (9) describes the Higuchi kinetic model, which states that the amount of medication released is proportional to the square root of time. (Marcos Luciano Bruschi, 2015)

$$M_t = K_H t^{1/2} \quad (9)$$

Where M_t is the amount of drug released at time t, and K_H is the Higuchi constant.

The Hixson–Crowell model, denoted by (Eq. (10)), describes that a cluster of particles' area is proportional to the cube root of its volume: (Marcos Luciano Bruschi, 2015)

$$\sqrt[3]{W_0} = \sqrt[3]{W_i} + K_{HC} t \quad (10)$$

The drug's initial concentration in the system is denoted by W_0, its remaining concentration on time t is indicated by W_i, and the constant of incorporation, K_{HC}, is used to relate surface and volume.

2.8. Antibacterial activity determination

2.8.1. Microbial strain and inoculum preparation

The microorganisms *Staphylococcus aureus*, *Escherichia coli*, *Klebsiella pneumoniae,* and *Pseudomonas aeruginosa* were procured from Medical Research Institute, Sri Lanka. To prepare the inoculum, each bacterial strain was cultured in a Luria Bertani broth at 37 °C overnight. For the antibacterial activity and minimum inhibitory concentration determination, a 24-hour aged bacterial culture was adjusted to obtain $five \times 10^5 CFU/mL$ with a 0.5 McFarland turbidity standard using a UV–visible spectrophotometer for subsequent analysis (Jayanetti et al., 2024).

2.8.2. Sample preparation

To determine the antibacterial activity, three concentrations, 5 mg/mL, 10 mg/mL, and 20 mg/mL were used from curcumin, chitosan, and composite samples. Then, 1 mL of DMSO was added to each sample and sonicated at 35°C for 90 min. These samples that were dissolved in DMSO were used to assess the antibacterial activity using the well diffusion method.

2.8.3. Well diffusion method

Adjusted bacterial suspension of 5×10^5 colony-forming units (CFUs)/mL in the Luria Bertani broth medium was inoculated to sterile Mueller–Hinton agar (MHA) plates through streaking. Wells were made in the MHA using a sterile cork borer, and a concentration series (5 mg/ml, 10 mg/ml, and 20 mg/ml) of each material was inoculated to the wells (Balouiri et al., 2016). Amoxicillin and DMSO were used as the positive and negative controls, respectively. Control of distilled water and ethanol was also used. Three replicates for each sample and each species of bacteria were prepared. After 18 h of incubation at 37 °C, inhibition zones were measured in mm (Al-Abdallah et al., 2022b; Sak et al., 2022; Shaaban et al., 2022).

2.8.4. Determination of minimum inhibitory concentration (MIC) and minimum bacterial concentration (MBC)

The antibacterial agents prepared were diluted into various concentrations ranging from 0.625 mg/mL – 20 mg/mL and a control concentration of 0 mg/mL in sterile Eppendorf tubes. Using a micropipette, 1 mL of each microbial culture of 0.5 McFarland standard was inoculated into test tubes containing 1 mL of the various concentrations of the antibacterial agent in Luria Bertani broth for determination of MIC. By performing a serial dilution of the samples in DMSO and plating them on nutrient agar plates, MBCs were determined. More precisely, Muller Hinton agar plates were inoculated with two µL of the test samples and the test organism from each test tube to determine MBC. The Muller Hinton agar plate used as a control had no test sample additions. After that, the test tubes and the plates were both incubated for 18 to 24 h at 37 °C, and the growth of bacteria and viable count were then monitored, respectively (Andrews, 2001; Hamama et al., 2018;

Jayanetti et al., 2024).

The concentration at which there was no discernible turbidity was identified as the minimum inhibitory concentration (MIC) of the test sample. On spread plates, MBC was shown to be the lowest concentration of sample, inhibiting the growth of bacteria and giving three log reductions (99.9 %).

2.9. Statistical analysis

Data from each experiment were statistically analyzed using SPSS Statistics (Version 27, SPSS Inc., Chicago, Illinois, USA), and results were expressed as mean ± standard error (SE). The confidence level of 95 % was set as the Statistical significance. One-way analysis of variance (ANOVA) was used to determine the differences among the treatment means.

3. Results and discussion

3.1. Characterization

3.1.1. XRD analysis

The XRD patterns were collected to study the crystallographic orientation of turmeric powder, synthesized chitosan, and the synthesized composite material (Fig. 1). The XRD pattern of the chitosan shows a significant peak at 19.47° which is attributed to the (1 1 0) crystalline plane pattern and the shoulder peak at 20.91°, which represents the (1 2 0) crystalline plane, and the small broad peaks at 23.46°and 26.36° correspond to the (1 0 1) and (1 3 0) crystalline planes of chitosan, respectively (Mendis et al., 2023). The d spacing values calculated by Bragg's law using Eq. (11) of the respective crystalline planes are 0.4555, 0.4220, 0.3807, and 0.3355 nm, respectively.

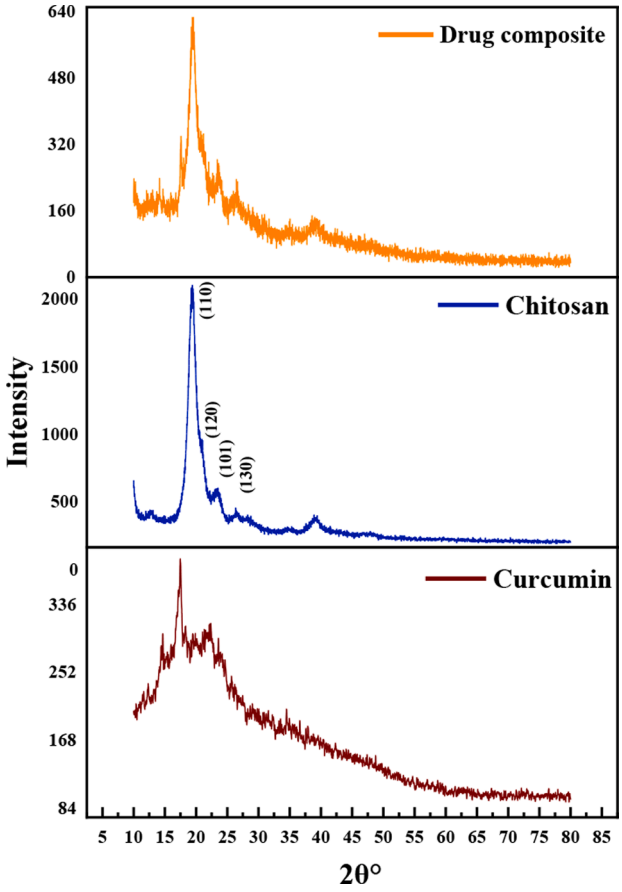

Fig. 1. XRD patterns of the materials.

The XRD pattern of curcumin shows peaks at 14.66°, 17. 20°, 18.36°, 19.9°, 22.1° 23.48° and 25.66° matching with the CCDC No. 82–8842 and JCPDS 9–816 (Van Nong et al., 2016). The inter-layer distances corresponding to the respective atomic planes are 0.5999, 0.5151, 0.4026, 0.4784, 0.4448, 0.3710, and 0.3430 nm, respectively.

The peak at 19.55° of the XRD pattern of the curcumin-chitosan composite, which corresponds to the (1 1 0) crystalline plane of chitosan, indicates the presence of chitosan in the composite and the presence of peaks corresponding to curcumin appear at 23.35°, 26.55°, 37.12°, 17.20° and 14.66° in the XRD pattern of the composite confirms the presence of curcumin crystallized on chitosan in the composite. The calculated d spacings values of the respective crystalline planes are 0.4537, 0.38070, 0.3355, 0.242, 0.5151, and 0.5999 nm, respectively.

The crystallite size was calculated by the Scherrer equation given in Eq. (12), using the highest intense peak of curcumin, chitosan, and the composite located at 2θ values of 17.20°, 19.47° and 19.55°.

$$\lambda = 2d\sin\theta \tag{11}$$

$$L = \frac{K\lambda}{\beta\cos\theta} \tag{12}$$

Where λ represents the wavelength of the X-ray source; θ: diffraction angle; L: crystallite size; β: half maximum of the peak in radians; K: Scherer's constant (0.89).

Table 1 summarizes the parameters related to crystalline structures. Curcumin was crystallized on the surface of chitosan during the preparation of the composite, resulting in the growth of the crystallite size, as evidenced by the increase in the crystallite size and the number of planes of the composite material in XRD results.

3.1.2. Scanning electron microscopy

SEM images were collected to study the 3D geometry of the surface of the prepared materials. A well-established oval-shaped macropore structure was established on chitosan, with the removal of protein present in the chitin upon treatment with 3 % NaOH (Fig. 2 (a)). In the composite, the macropore structure is disturbed by the crystallization of curcumin on the porous structure of chitosan, as shown in the SEM image in Fig. 2 (b).

3.2. Egg albumin denaturation assay

Curcumin extract has a substantial anti-inflammatory property, as shown in Fig. 3 (a). Curcumin extract has acted in a dose depending on manner in the range of 100 µg/ml to 1600 µg/ml. The composite, which consists of curcumin extract and chitosan, has been shown to possess strong anti-inflammatory capabilities due to the grafting of curcumin onto the surface of the delivery system. The IC_{50} values of curcumin and composite materials are 0.285 mg/ml and 1.083 mg/ml, respectively. Lower IC_{50} values indicate higher activity against the inflammatory reactions (Elisha et al., 2016). Further, it can be concluded that the ethanolic extract of the turmeric powder consisting of phytochemicals such as polyphenols, terpenoids, and flavonoids (curcumin)(Gonfa et al., 2023) has contributed to the substantial anti-inflammatory potential and has been expressed in the developed novel delivery system.

Steroid and nonsteroidal anti-inflammatory drug therapy is the conventional method of treating inflammatory diseases. However, these medications can have serious side effects like myocardial infarction (Truong et al., 2019). Therefore, with minimal probability of causing

Table 1
Crystallographic parameters were calculated from XRD data.

Sample	2θ°	L (nm)	d (nm)	L/d
Curcumin	17.20	28.47	0.5151	55.27
Chitosan	19.47	55.01	0.4555	120.77
Composite	19.55	66.11	0.4537	145.71

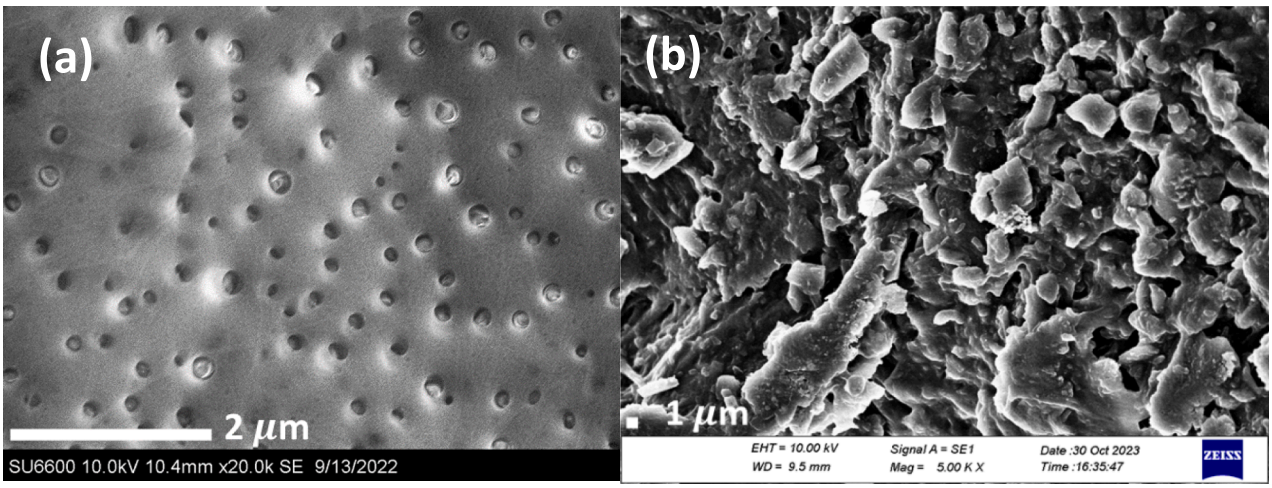

Fig. 2. SEM images of (a)Chitosan (b)Chitosan-curcumin composite.

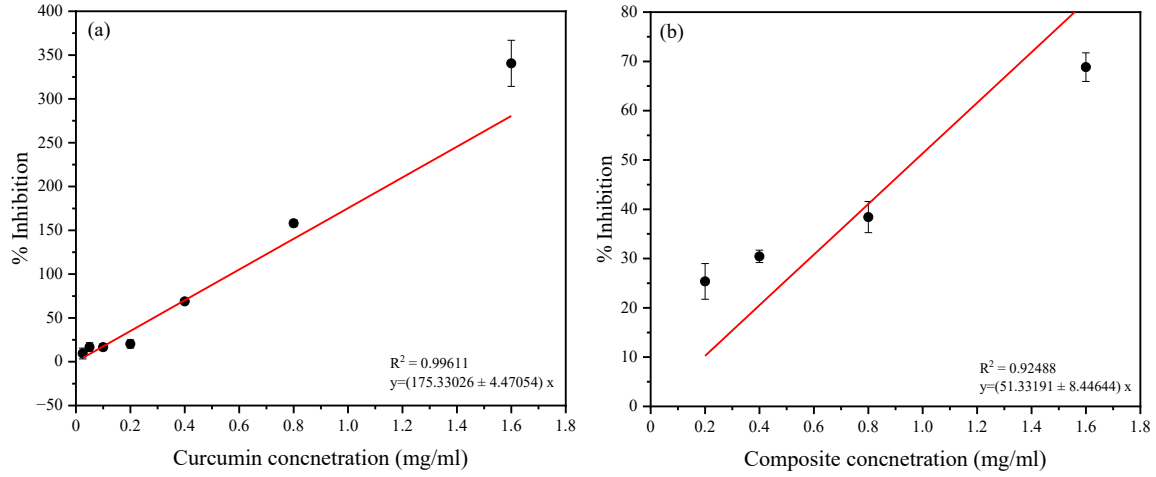

Fig. 3. Anti-inflammatory activity of (a) curcumin extract (b) curcumin chitosan composite.

adverse drug reactions, curcumin-loaded chitosan composites can act as a potential plant-based drug to replace synthetic drugs due to their substantial anti-inflammatory activity.

3.3. DPPH radical scavenging ability

When endogenous reactive oxygen species, or ROS, generation exceeds the body's antioxidant capability, oxidative damage typically

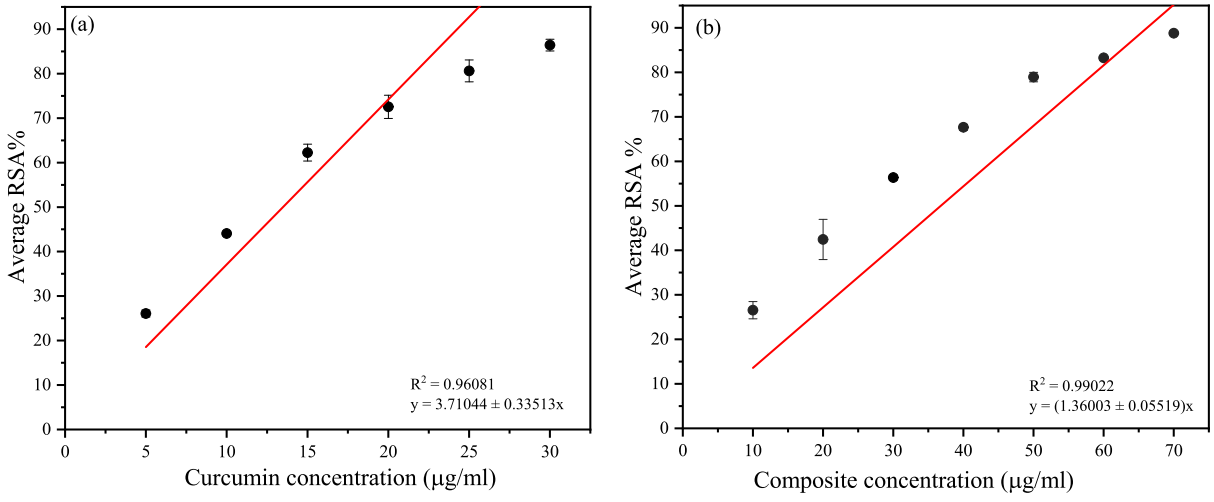

Fig. 4. DPPH antioxidant assay (a) curcumin (b) drug composite.

occurs (Shaaban et al., 2021). As a well-known potent antioxidant, curcumin has shown a dose-dependent increment in the RSA% with the concentration. According to Fig. 4, the radical scavenging ability has reached a saturated level (80.62 ± 2.45 %) when the concentration is above 25 $\mu g/ml$, where it no longer represents a linear behavior. As the linear range of the RSA% was not prominent for higher concentrations (>25 $\mu g/ml$), curcumin's antioxidant potential was determined over a concentration range of 5——25 $\mu g/ml$. For the composite, a concentration series of 10——70 $\mu g/ml$ was used where the RSA% reached the maximum value of 88.78 ± 0.32 % at 70 $\mu g/ml$ in the concentration series tested. From 10 − 70 μg/ml, the RSA% varied from 26.57 ± 1.94 to 88.78 ± 0.32, acting in a dose-dependent manner. The IC_{50} values of curcumin and composite materials were determined to be 13.47 μg/ml and 36.76 μg/ml, respectively. Ascorbic acid was used as the positive control, and the values obtained were significantly higher than those of the composite samples. At 50 μg/ml, the composite showed 78.93 %, whereas the positive control showed 91.66 % DPPH radical scavenging activity.

The IC_{50} of the novel composite is mainly attributed to the high DPPH radical scavenging ability of the bioactive curcumin, which has been grafted upon chitosan biopolymer. Sánchez-Machado et al. (Sánchez-Machado et al., 2018) and Tomida et al.(Tomida et al., 2009) have reported that chitosan also possesses antioxidant activity.

Anraku et al.(Anraku et al., 2008) indicate that chitosan exhibits antioxidant properties at varying molecular weights. Human serum albumin is protected from oxidation by low molecular weight chitosan by inhibiting the production of carbonyl and hydroperoxide groups (Anraku et al., 2008). Curcumin is a lipid-soluble substance with antioxidant activity that can bind to the cell membrane and gets transformed into phenoxyl radical by seizing the action of lipid radicals. Thereafter, penoxyl radicals can be restored by water-soluble substances such as ascorbic acid after moving to the cell membrane surface. This transformation is facilitated by the higher polarity nature of the phenoxyl radicals than that of curcumin (Ak & Gülçin, 2008; Jovanovic et al., 1999). The study conducted by Priyadarsini et al.(Priyadarsini et al., 2003) has provided experimental and theoretical outcomes that collectively affirm curcumin's superior antioxidant effectiveness, primarily resulting from its phenolic OH group, with a minor role played by the CH_2 site. Further, the phenolic OH group in curcumin hinders lipid peroxidation induced by free radicals and exhibits antioxidant qualities (Priyadarsini et al., 2003).

Therefore, both the curcumin and chitosan's antioxidant ability have resulted in a higher antioxidant potential in the composite material. Both the samples showed an intense colour change over the concentration, where the purple colour at low concentrations converted to light yellow colour at higher concentrations of the sample.

3.4. Drug release and statistical analysis

A one-way ANOVA test was conducted to determine the differences in the percentage of cumulative drug release (%CDR) with varying pH levels and ionic strengths of the release media. The results are summarized in Table 2 (A) and Table 2. (B). Table 3..

According to the results, the pH ranges from pH 1 – 4 have shown a significant difference in the % CDR profile with that of the media with pH 7.4 (p-value < 0.05). This can be further confirmed by the significant F values reported in the pH range of 1–4. However, in the pH range from 5.5 to 8.5, the drug release profile does not show a significant difference with that of pH 7.4 (p-value > 0.05). When the pH is increased to 10 drug release behaviour was changed significantly concerning that in pH 7.4 (p-value < 0.05, significant F value). These behaviours correspond to the structural differences and breakdown of the curcumin with the change of the pH in the release medium. Further, it can be seen from the % CDR values that were recorded for 10 h that the drug release increased with increasing alkalinity of the release medium, in which the best release profile over time was obtained at pH 10. Since the mode of administration of the drug delivery systems is either the oral or the intravenous (IV) routes, pH values higher than 7.4 were not taken into consideration when analyzing the results with kinetic models, even though the %CDR was higher. Furthermore, at pH > 7 conditions, curcumin breaks down in 30 min to produce vanillin, 4-dioxo-5-hexanal, ferulic acid, feruloylmethane, and Trans-6-(40-hydroxy-30-methoxyphenyl)-2 (W. Liu et al., 2016). Curcumin breaks down much more slowly in acidic environments; after one hour, less than 20 % of the total curcumin had broken down, as depicted by Cas & Ghidoni (Cas & Ghidoni, 2019) and W. Liu et al.(W. Liu et al., 2016). Moreover, the blood pH is known to be 7.4 in general conditions. Therefore, pH 7.4 media was taken as the media with a higher % CDR for further analysis. Sodium chloride was used to change the ionic strength of the medium, and the %CDR of the media with molarity ranging from 0.1 M−0.5 M was compared with that of 0.3 M. All the release profiles were shown to be significantly different at the 95 % confidence interval when compared to that resulted with 0.3 M NaCl. A better release profile was obtained for the 0.3 M NaCl concentration, and %CDR was found to decrease when the NaCl concentration was increased further. According to Jafari et al. (Jafari et al., 2023), the concentration range of 0.1 M – 1 M NaCl has affected the stability of the curcumin nanoemulsion. Nanoemulsion aggregates in media with higher ionic strength because the electrostatic repulsion between the particles tends to be superseded by the more prominent attractive forces such as van der Waals and hydrophobic interactions. They further indicate that the zeta potential of the nanoemulsions was decreased drastically (near 0) at the higher NaCl concentrations, which in return facilitated the destabilization of nanoemulsion by overcoming the electrostatic repulsion. Conversely, at lower NaCl concentrations, electrostatic repulsion dominated the weaker van der Waals forces and hydrophobic interactions of the nanoemulsions. Peng et al. 2018) indicated that nanoparticles are stabilized against aggregation at NaCl concentrations lesser than 500 mM, but at NaCl concentrations of 500 mM − 1000 mM, nanoparticles tend to aggregate because of the strong, attractive forces compared to the electrostatic repulsions. In the current study, ionic strength varied in a range below 500 mM, and the media with the best-released profile was used for further analysis. Supporting these facts, a media consisting of a pH of 7.4 and 0.3 M NaCl concentration was prepared to assess the drug release profile of the drug with changing the drug dosage (2.5 mg – 10 mg).

Even though curcumin exhibits anti-oxidant, anti-inflammatory, particularly anti-neuroinflammatory, anti-tumor, antithrombotic, immunomodulatory, antidiabetic, analgesic, and microglia-activation inhibitory effects (Bagheri et al., 2020), curcumin cannot be used as a

Table 2B
ANOVA results in Average %CDR of varying NaCl concentrations compared with the %CDR of the media having 0.3 M NaCl ionic strength.

NaCl conc:	0.1 M	0.2 M	0.4 M	0.5 M
F-value	7.0450	31.4020	14.9270	5.7210
p-value	0.0100	0<.001	0<.001	0.0190

Table 2A
ANOVA results Average %CDR of varying pH values compared with the %CDR of pH 7.4.

pH	1	2.5	4	5.5	7	8.5	10
F-value	5.6240	22.6000	20.2060	0.0360	2.6910	0.0490	182.3250
p-value	0.0200	0<.001	0<.001	0.8510	0.1050	0.8260	0<.001

Table 3
Antibacterial activity of curcumin, chitosan and CCC.

Sample/Concentration	Zone of Inhibition (mm) ± SE			
	Pseudomonas aeruginosa	***Klebsiella pneumoniae***	***Staphylococcus aureus***	***Escherichia coli***
5 mg /mL				
Curcumin	10.67 ± 0.67	11.50 ± 1.04	12.34 ± 0.34	0
Chitosan	11.00 ± 0.58	10.00 ± 1.22	0	11.75 ± 0.61
Composite	11.67 ± 0.88	12.00 ± 0.76	13.34 ± 0.34	0
Amoxicillin	29.30 ± 0.12	25.40 ± 0.87	40.50 ± 0.73	39.50 ± 1.21
10 mg /mL				
Curcumin	10.84 ± 0.44	11.84 ± 1.01	15.67 ± 0.67	0
Chitosan	11.67 ± 1.20	11.67 ± 0.17	0	13.17 ± 1.77
Composite	10.84 ± 0.60	10.67 ± 0.67	16.34 ± 0.60	0
Amoxicillin	30.00 ± 0.98	25.00 ± 0.81	21.50 ± 1.31	20.00 ± 0.98
20 mg /mL				
Curcumin	09.67 ± 0.34	11.67 ± 0.34	12.84 ± 0.60	0
Chitosan	13.00 ± 1.32	11.00 ± 0.58	0	12.17 ± 0.60
Composite	10.84 ± 0.44	11.00 ± 0.58	13.34 ± 0.73	0
Amoxicillin	31.50 ± 0.97	26.00 ± 1.23	24.00 ± 1.03	24.00 ± 0.75

direct medication orally or intravenously because of its' poor pharmacokinetic properties. The primary objective of developing a delivery system for curcumin is to enhance pharmacokinetic properties compared to free curcumin (Fig. 5). Because of the positively charged nature of the chitosan biopolymer, it can open the epithelial cell tight junctions of the mucous membrane (Choukaife et al., 2022) to deliver

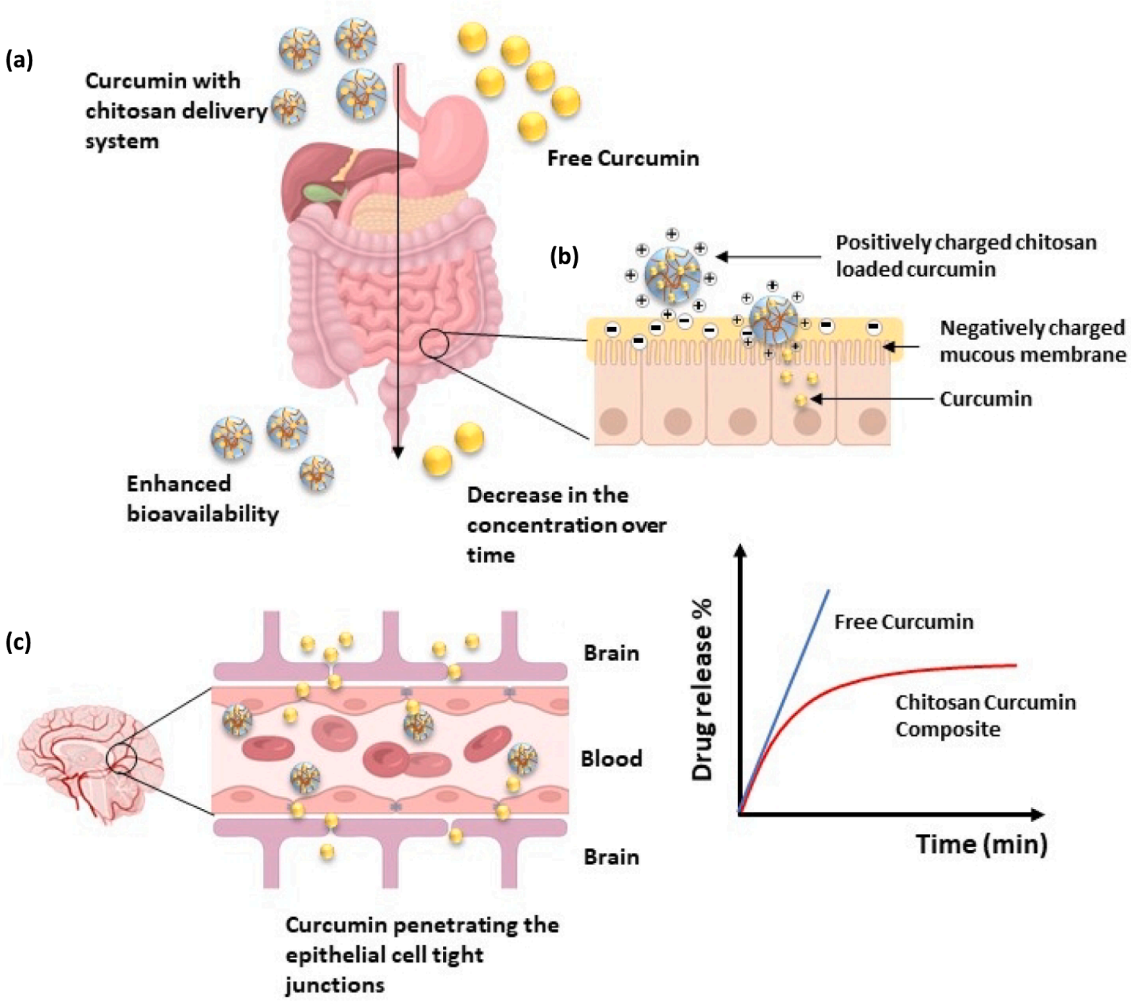

Fig. 5. Drug composite's pharmacokinetic properties (a) Enhanced bioavailability of chitosan-curcumin drug composite over time in the gastrointestinal tract (b) Schematic representation of drug composite structure and interaction with the mucus layer (c) Curcumin penetrating the epithelial cell tight junctions in the blood–brain barrier.

the curcumin to the target sites effectively when administrated orally, as shown in Fig. 5 (b). Due to its pleiotropic therapeutic properties on the neurological system, curcumin has been considered a possible therapeutic factor for a wide range of central nervous system-associated diseases. Curcumin can also pass the blood–brain barrier (BBB) (Mirzaei et al., 2017; Yavarpour-Bali et al., 2019). Numerous experimental and clinical investigations have demonstrated the beneficial effects of curcumin in neuroinflammatory illnesses, such as Alzheimer's disease (Hamaguchi et al., 2010b), Multiple Sclerosis (Xie et al., 2011), and Parkinson's disease (B. et al. Bharath, 2012). Therefore, the suggested novel drug delivery system possesses the ability to deliver curcumin to the brain target tissues as well (Fig. 5 (c)). Upon uptake of the drug intravenously or orally, the cellular lifespan of the drug composite is shown in Fig. 6. Following the endocytosis of the curcumin-loaded chitosan drug composite by cells, endosome complexes are formed, entrapping the drug molecules. An endosome/lysosome hybrid is formed with the fusion of lysosome to this complex, which, in return, is responsible for the release of the drugs to the cytoplasm by digestion and rupturing the hybrid complex. Subsequently, the release of curcumin to the extracellular matrix is driven by higher Ca^{2+} levels in the extracellular space (Liang et al., 2021). Considering these therapeutic potentials, the release of the drug from the delivery system can be assessed through an *in vitro* study to confirm whether the incorporation of a chitosan biopolymer-based delivery system has improved the pharmacokinetic properties of curcumin.

All the experimental drug release data are fitted into kinetic models considering only the first 60 % of the drug release. Supplementary Table 1A, Table 1B, and Table 1C summarize the model parameters of each of the six models used in the study. Considering the R^2 values ($R^2 >$ 0.99) of the model fits, KP and PS models were selected to explain the release mechanism of the curcumin-coated chitosan composite material. Linear models like first order, zero order, and HC models were not taken into consideration when interpreting the results because of the lower R^2 values obtained for the fitted % CDR data ($R^2 < 0.95$).

Supplementary Table 1A, Table 1B, and Table 1C show the model parameters of the KP model, which are attributed to the n: diffusional exponent and k_p: release constant about the curcumin release from the chitosan polymeric matrix. According to the parameter "n," the model offers information about the release profile that can be either a Fickian distribution (Case I) or a non-Fickian distribution (Case II, Anomalous Case, and Super Case II). (Ritger & Peppas, 1987) (Ritger & Peppas, 1987)state that the Fickian diffusion controls the drug release mechanism when $n = 0.43$, anomalous (non-Fickian) transport occurs when $0.43 < n < 0.85$, and case II transport occurs when $n = 0.85$ (Marcos et al., 2015; Unagolla & Jayasuriya, 2018). These n values explained by the KP model apply to samples of monodispersed polymers; however, Ritger & Peppas (Ritger & Peppas, 1987) and Unagolla & Jayasuriya (Unagolla & Jayasuriya, 2018)reported that n values of approximately 0.3 ± 0.1 in polydisperse spherical samples are also feasible for Fickian diffusion. The n values obtained in this study for all the varied parameters are approximately 0.30 ± 0.01, which is less than 0.43 and hence propose the occurrence of the Fickian diffusion mechanism in polydispersed polymer matrices. Fig. 7 indicates the Ritger-Peppas model's nonlinear curve fitting to the obtained experimental data. The physical and structural characteristics of the drug and polymer matrix both affect the release constant (k_p), which is directly proportional to the diffusion constant (Unagolla & Jayasuriya, 2018). As shown in Supplementary Table 1A, Table 1B, and Table 1C, the highest kp value was obtained in media consisting of a pH value of 10, 0.3 M NaCl concentration, and a drug dosage of 2.5 mg. While pH ten has shown a higher release rate, pH 7.4 has also exhibited a better release rate over time, as discussed under 3.5.

The PS model considers both the Fickian contribution and the case II relaxation contribution (second term of Eq. (7)) (Marcos et al., 2015). The purely Fickian diffusion exponent is related to the exponential coefficient m. The values of n and m in Eqs. (6) and (7) should be equal if the relaxational mechanism is insignificant (Abdul Hameed et al., 2020; Marcos et al., 2015; Unagolla & Jayasuriya, 2018). Therefore, the difference between the n and m exponents indicates that case II relaxation, as well as Fickian diffusion, are important mechanisms in the curcumin release process from chitosan. The relaxational over Fickian contribution ratio can be computed using Eq. (8). Supplementary Fig. 1 represents the Fitted %CDR data, and supplementary Fig. 2 shows the variation of R/F values of the Peppas-Sahlin model. Supplementary Figs. 3, 4, 5, and 6 show the variation of Fitted %CDR data of Higuchi, Zero order, First order, and Hixson–Crowell models.

Fig. 2 displays the variation of the R/F ratio against time in different media conditions. The extremely low R/F values initially show that the Fickian diffusion governs the drug release during 0–30 min at some media compositions. It is observed that the relaxation mechanism contributes to the release of curcumin from chitosan biopolymer over time, as depicted by the increase in the R/F values. When R/F is equal to 1,

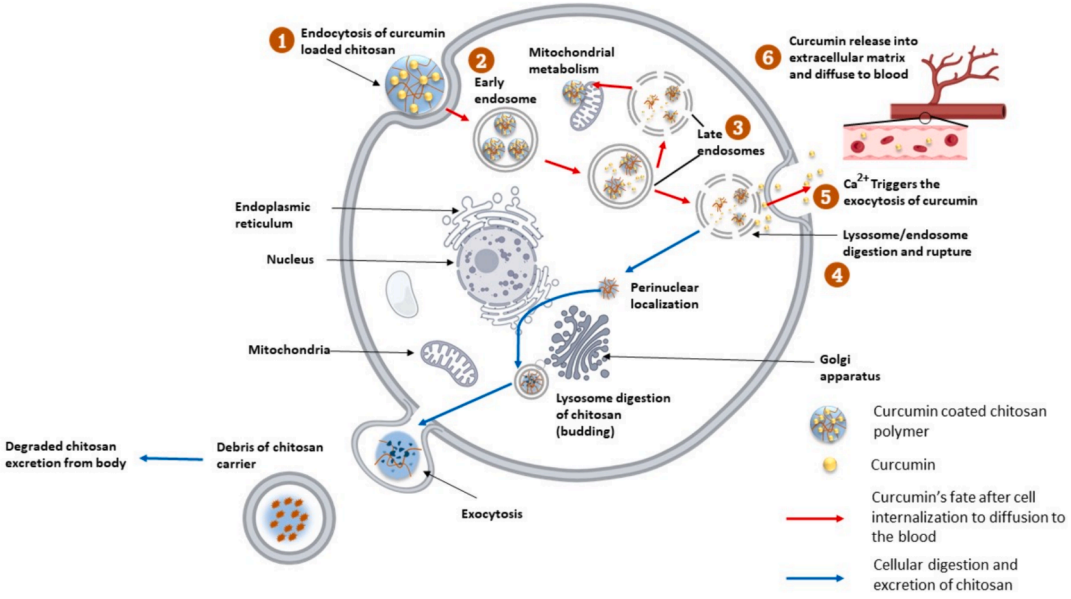

Fig. 6. Cellular lifespan of the drug composite.

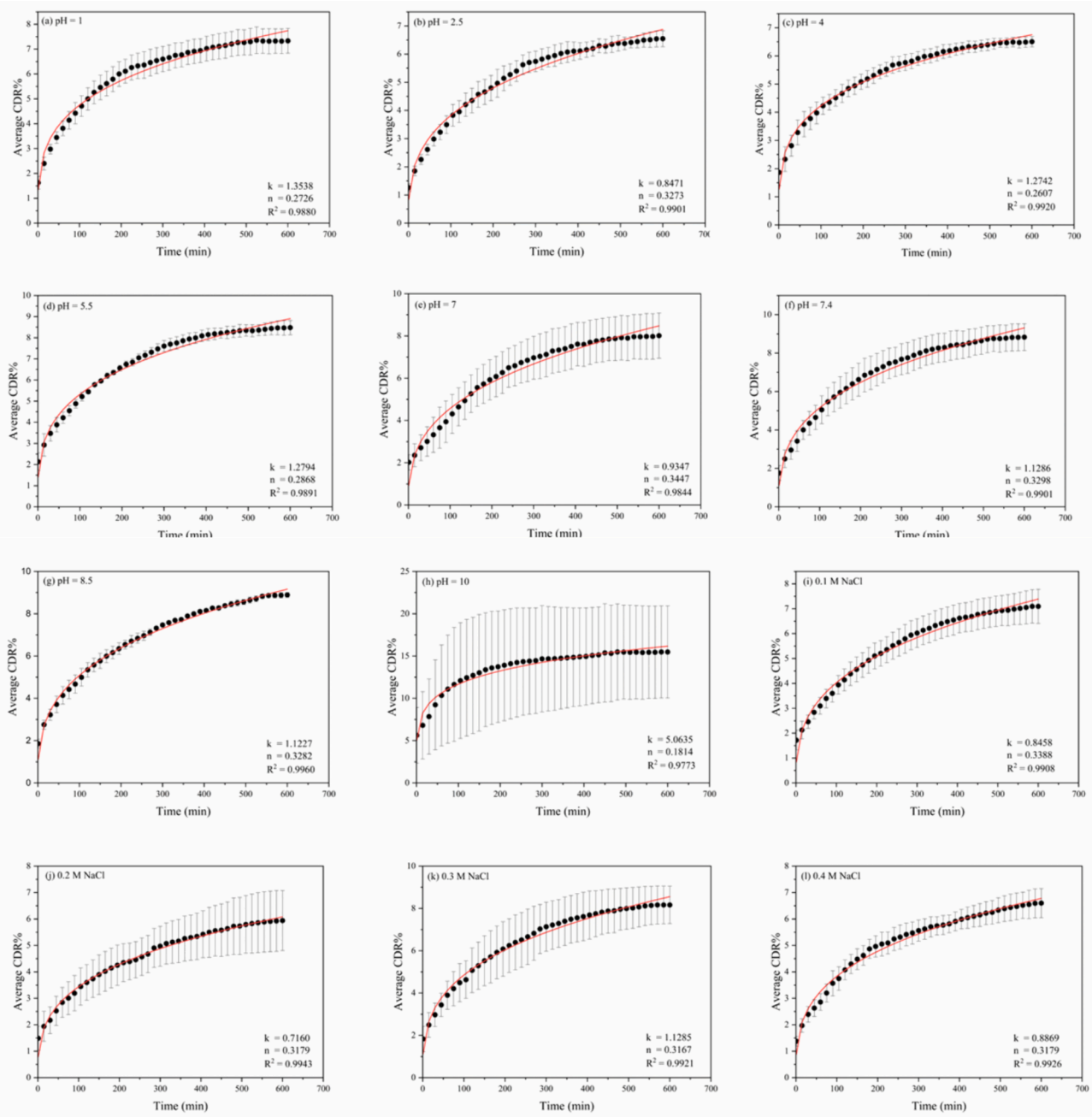

Fig. 7. Fitted %CDR data for Korsmeyer–Peppas model of the drug composite under varying media conditions; (a-h) pH,(i-m) ionic strength,(n-q) drug concentrations.

erosion and diffusion equally contribute to the release of curcumin, where diffusion predominates when $R/F < 1$, and relaxation (erosion) predominates when $R/F > 1$ (Jadidi et al., 2020).

Peppas-Sahlin model indicates higher rates of curcumin release (k_D and k_R) in media with pH 10, 0.3 M NaCl, and 2.5 mg of curcumin-chitosan composite, separately, being similar to the KP and Higuchi models, suggesting significantly higher release of curcumin under those conditions. Curcumin release at pH 1 deviated where polymer relaxation did not play a major part in drug release ($m = n$), where polymer relaxation had proven to play a predominant role in the release of the curcumin from the drug when the pH was increased. Low R/F values at the beginning of the release (less than 0) gradually increased over time until pH 7.4, suggesting that diffusion predominated in the first phase of the drug release (0–30 min) and with time relaxation became more prominent. In the media with the highest ionic strength (0.5 M), polymer relaxation has not been a mechanism in releasing the curcumin ($R/F < 0$), which can be further proven by the $m = n$ value in Supplementary Table 1(B). Therefore, it is suggested that the increase in the NaCl concentration aggregation of the drug composite might have hindered the relaxational mechanism. At pH 1, curcumin might not have been released effectively due to its' weaker degradation at an acidic medium ($R/F < 0$). Jafari et al.(Jafari et al., 2023) indicated that the particles tend to aggregate as the surface electrical charge of the particles reduces the electrostatic repulsive forces at lower pH values, which might have contributed to the lower release of curcumin at low pH. However, it should be emphasized that the Fickian diffusion was actively responsible for the release of the curcumin in all the cases.

The Higuchi model is not theoretically applicable to the analysis of

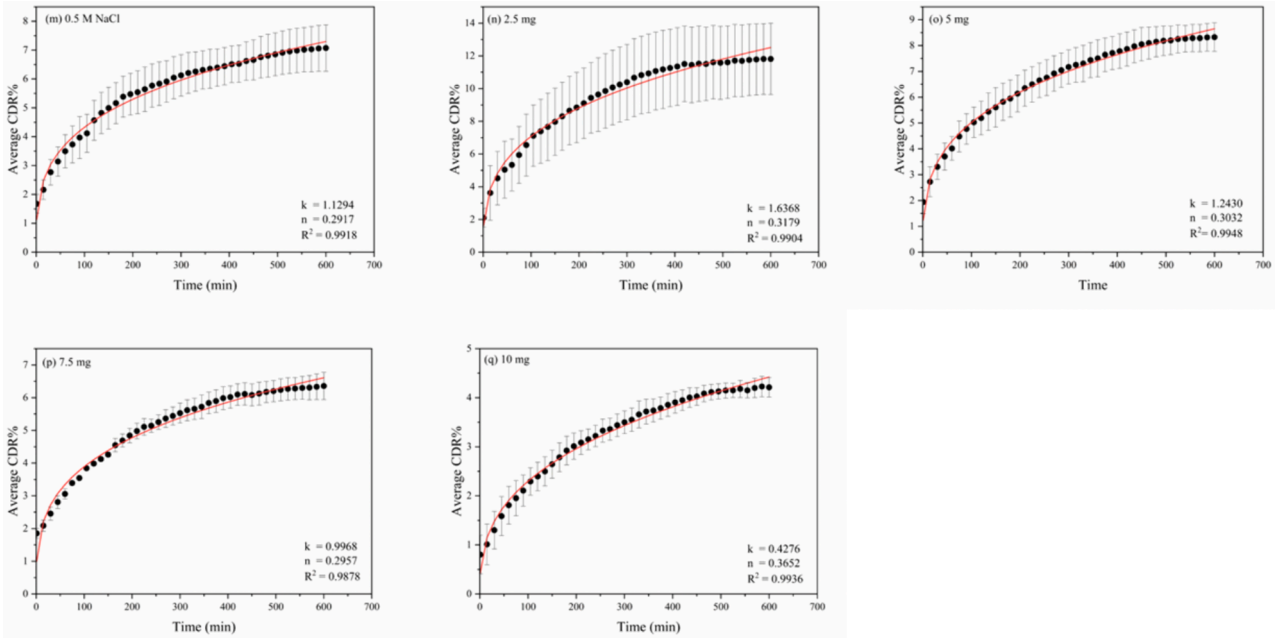

Fig. 7. (*continued*).

swellable drug delivery systems because the model discusses only the effect of time on the release. As this model completely neglects the swelling or dissolution effect of the polymeric carrier system in its' basic assumptions, using this model alone for the analysis can lead to erroneous conclusions on the drug delivery mechanism (Peppas & Narasimhan, 2014). Nonetheless, the model has been frequently applied in swellable polymer systems to provide a general understanding of the drug transport mechanism because of its incredibly simple nature. In a diffusion-controlled drug delivery system, proportionality between the CDR and the squared of time is seen to be a reliable metric for studying drug release. Consequently, if the Higuchi model is applied, more mathematical analysis must be required to conclude the drug release mechanism (Peppas & Narasimhan, 2014; Siepmann & Siepmann, 2008).

HC model discusses drug release when it dominates by dissolving velocity instead of diffusion. In the current drug delivery system, diffusion has proven to be the major factor in the release of drugs according to the higher R^2 values reported for the KP model, which is further proven by the lower R^2 values obtained for the HC model and therefore, can be concluded that curcumin is not released from the chitosan matrix by dissolution solely (Rostami et al., 2014).

The reservoir diffusion-type drug delivery system is reflected in both the first-order and zero-order models (Wójcik-Pastuszka et al., 2019). Case II transport is assumed in the zero-order model (Marcos et al., 2015). Furthermore, the first order is theoretically equal to the KP model in the cases where $n = 1$, indicating that the case II transport mechanism is the responsible factor for the drug release (Unagolla & Jayasuriya, 2018). Supplementary Table 1 (A), Table 1 (B), and Table 1 (C) exhibit lower R^2 values for zero and first order, indicating inadequate fitting of the experimental data. Thus, case II transport does not entirely cause curcumin release from chitosan.

In summary, both the Fickian diffusion and polymer relaxation (case II) transport play govern the release of curcumin from chitosan over time according to non-linear curve fitting data reported in the *in vitro* study.

3.5. Antibacterial activity

According to the results shown in Fig. 8 (a) and (b), both curcumin and composite material have shown antibacterial activity against *Pseudomonas aeruginosa, Klebsiella pneumoniae, and Staphylococcus aureus*. Out of all three samples, curcumin extract, chitosan, and composite, chitosan was effective against only *Pseudomonas aeruginosa*, *Klebsiella pneumonia*, and *Escherichia coli* bacterial strains. Among these three bacterial strains, chitosan was highly effective against *Escherichia coli*, resulting in zones of inhibition of 11.75 ± 0.61 mm, 13.17 ± 1.77 mm, and 12.17 ± 0.60 mm for 5 mg/mL, 10 mg/mL, and 20 mg/mL concentrations respectively. The zones of inhibition against *Pseudomonas aeruginosa* were reported to be 11 ± 0.58 mm, 11.67 ± 1.20 mm, and 13 ± 1.32 mm, while *Klebsiella pneumonia* showed 10.00 ± 1.22 mm, 11.67 ± 0.17 mm and 11.00 ± 0.58 mm for the three concentrations tested. However, chitosan did not show any antibacterial effect against the Gram-positive bacterial strain, *Staphylococcus aureus.*Fig. 9.

Among the four pathogenic microorganisms tested, *Staphylococcus aureus* was found to be the most susceptible to the inhibitory activity of curcumin extract and the newly synthesized curcumin grafted composite. In terms of varied concentrations of the curcumin extract and composite tested, 10 mg/mL was proven to have the highest antibacterial effects than 5 mg/mL and 20 mg/mL against *Pseudomonas aeruginosa*, *Klebsiella pneumonia*, and *Staphylococcus aureus*. The reported zones of inhibition of curcumin extract and composite material against *S.aureus* at 10 mg/mL were 15.67 ± 0.67 mm and 16.34 ± 0.60 mm, whereas the zones of inhibition of curcumin extract and composite material at 5 mg/mL were 12.34 ± 0.34 mm, 13.34 ± 0.34 mm and at 20 mg/mL the values were, 12.84 ± 0.60 mm and 13.34 ± 0.73 mm. Considering the given results, it was apparent that when the concentrations of the samples increased from 10 mg/mL to 20 mg/mL, zones of inhibition decreased, indicating that higher molecular weight and bulkiness of the chitosan polymer could have contributed to lowered diffusion of the extract in Mueller–Hinton agar medium and composite in the MHA growth media (Kong et al., 2010; Verlee et al., 2017).

The positive control Amoxicillin showed higher zones of inhibition than Curcumin, Chitosan, and Composite against all test microorganisms at 5 mg/ mL, 10 mg/ mL, and 20 mg/ mL. The highest zone of inhibition for Amoxicillin was recorded against *Staphylococcus aureus* with a zone of 40.5 ± 0.73 mm at 5 mg/ mL, whereas the same in Curcumin, Chitosan and Composite were 12.34 ± 0.34, 0 and 13.34 ± 0.34.

Moreover, the composite material has shown higher inhibitory activity against the most susceptible *S. aureus* than the curcumin extract itself. This indicates that the grafting of curcumin to chitosan has

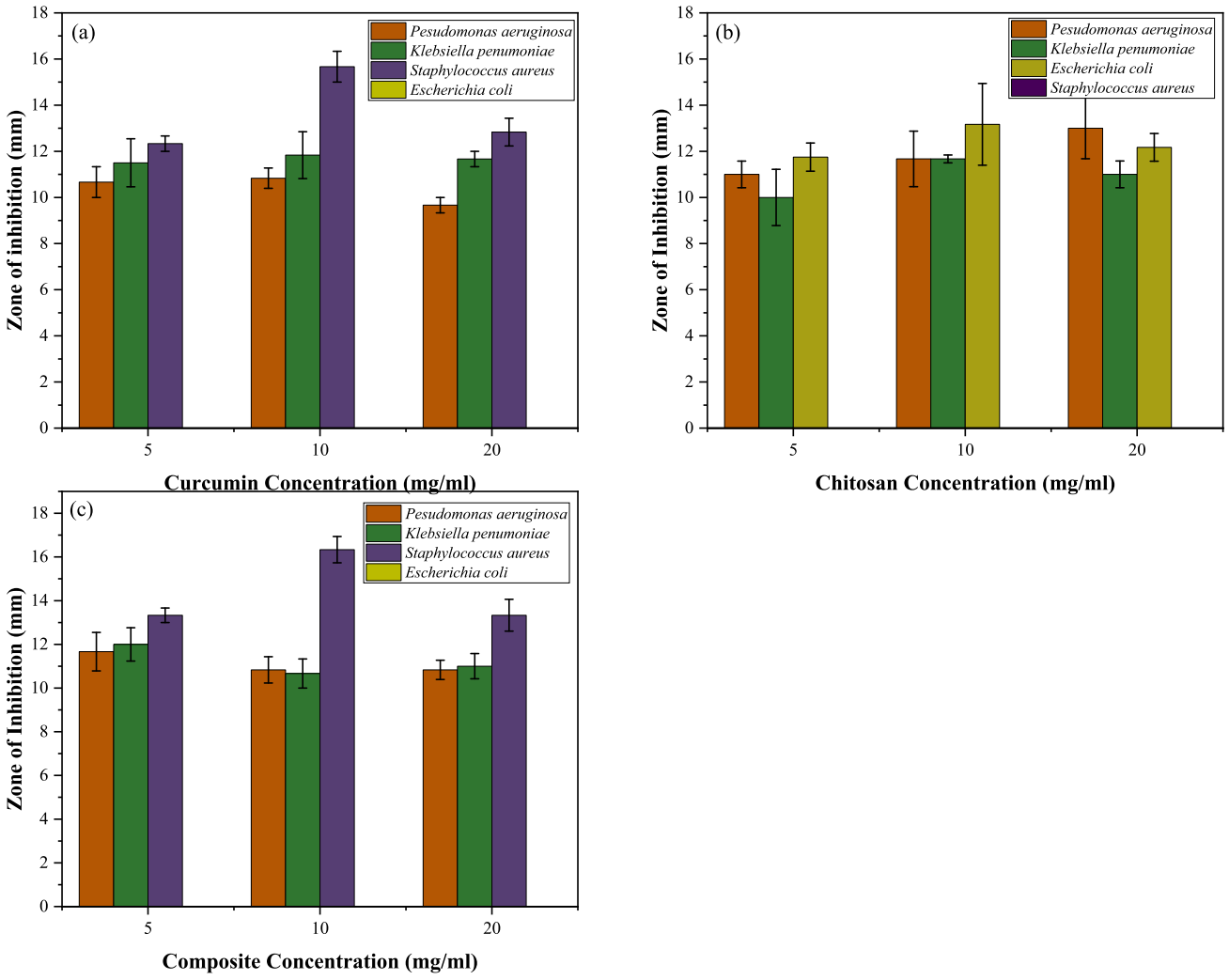

Fig. 8. Antibacterial activity of (a) curcumin and (b) chitosan (c) drug composite against *Pseudomonas aeruginosa, Klebsiella pneumoniae, Staphylococcus aureus* and *Escherichia coli.* *Footnote: The obtained zones of inhibition of curcumin, chitosan, and drug composite against Pseudomonas aeruginosa, Klebsiella pneumoniae, and *Staphylococcus aureus.*

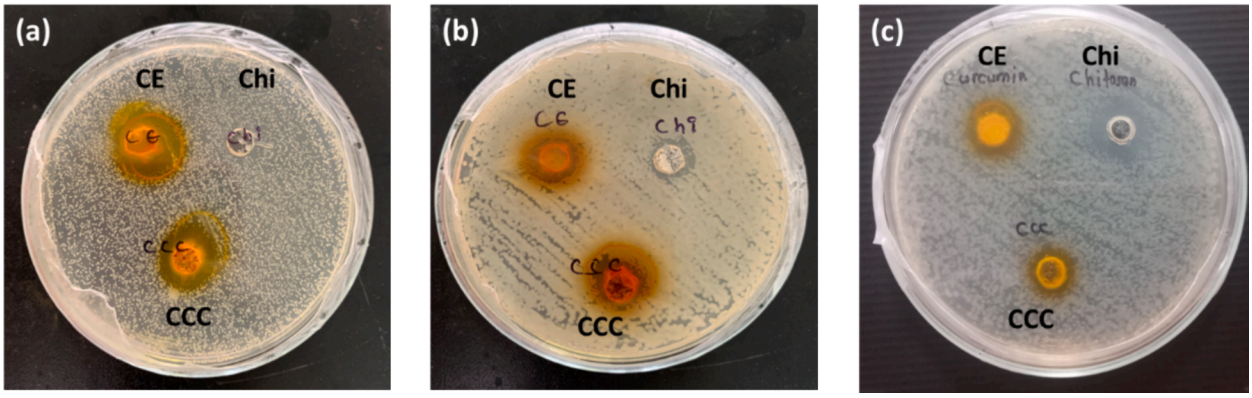

Fig. 9. Antibacterial activity of Curcumin extract (CE), Chitosan (Chi), and composite material against (a) Staphylococcus aureus, (b) Klebsiella pneumoniae, and (c) *Pseudomonas aeruginosa.*

significantly improved ($p < 0.05$) the bioavailability of the newly developed composite material, contributing to higher antibacterial activity. Since chitosan is a positively charged molecule, it often interacts well with negatively charged cell membranes (around − 70 mV) as a result of ionic exchanges mediated by the Na^+/ K^+ pump between the intracellular and extracellular medium. Because of the positive charge, the cells tend to absorb chitosan nanoparticles more frequently, increasing the biocompatibility of the drug (Rodrigues et al., 2012).

Between *K. pneumoniae* and *P. aeruginosa, K. pneumoniae* was more susceptible to both curcumin extract and composite. The zones of

inhibition that were reported for curcumin extract against *K. pneumoniae* were 11.50 ± 1.04 mm, 11.84 ± 1.01 mm, and 11.67 ± 0.34, while *P. aeruginosa* showed zones of inhibition of 10.67 ± 0.67 mm, 10.84 ± 0.44 mm, and 9.67 ± 0.34 mm at 5 mg/ mL, 10 mg mL, and 20 mg/mL concentrations, respectively. Enhanced antibacterial activity of composite material was observed at 5 mg/mL concentration against *K. pneumoniae* and *P. aeruginosa*, which is depicted by the zones of inhibition of 12 ± 0.76 mm and 11.67 ± 0.88 mm, respectively. When the concentration increased (>5 mg/mL), the zones of inhibition for the composite material against *K. pneumoniae* were 10.67 ± 0.67 mm and 11.00 ± 0.58 mm for the concentrations of 10 mg/mL and 20 mg/mL, respectively. Whereas for *P. aeruginosa,* it was reported to be 10.84 ± 0.60 mm and 10.84 ± 0.44 mm, respectively.

No zones of inhibition were reported for curcumin and composite material against the *E. coli* in the tested concertation range. The structure of the outer membrane of *E. coli* consists of outer membrane proteins (OMPs) that can act as selective channels to regulate the molecule uptake into the cells. Y. F. Liu et al.(Y. et al. et al., 2012) and Azucena et al.(Azucena et al., 2019) have indicated that curcumin does not show antibacterial activity against *E. coli* due to this complex cellular structure of Gram-negative bacteria. However, chitosan showed antibacterial activity against *E. coli* at the tested 5 mg/mL, 10 mg/mL, and 20 mg/mL concentrations due to the higher affinity and absorption of positively charged chitosan to the negatively charged cellular membrane of the gram-negative *E.coli*. Conversely, when curcumin is grafted onto the surface of the chitosan carrier, the net positive charge has been decreased. In comparison, fewer positively charged amino groups are usually available when chitosan is prepared as a carrier and combined with a drug. Its ability to interact with cell membranes and its surroundings is subsequently impacted by its reduced charge, which may limit its absorption and, ultimately, its potential toxicity (Rodrigues et al., 2012). The proposed antibacterial mechanism of the drug composite is shown in Fig. 10.

MIC and MBC results are reported in Table 4, where all samples except for curcumin against *K. pneumoniae* and chitosan against *S. aureus* showed bacteriostatic effects with MBC/MIC ≤ 4. The MIC and MBC assays offer essential information about the mode of action of an antibacterial agent. The lowest concentration of bactericidal activity of an antibacterial agent is known as the minimum bactericidal concentration or MBC. MIC is defined as the lowest concentration of a material that can inhibit the visible growth of an organism. The MBC/MIC ratios were determined to evaluate the mode of antibacterial activity. The MBC/MIC ratio ≤ 4 indicates the bactericidal effect, whereas MBC/MIC > 4 indicates the bacteriostatic effect (Jayanetti et al., 2024).

The effectiveness of curcumin as a bacteriostatic agent varies significantly among gram-positive and gram-negative bacteria due to the differences in the components of their cell walls and membranes. Curcumin may interfere with the protofilament polymerization process linked to the FtsZ protein, which is crucial in cell division in microorganisms (Yun & Lee, 2016).

Curcumin has had higher antibacterial activity against Gram-positive bacteria in comparison to Gram-negative bacteria (Adamczak et al., 2020; Azucena et al., 2019). In the current study, curcumin and the composite showed the highest antibacterial effects on *S. aureus.* Furthermore, curcumin damages the bacterial membrane to prevent *S. aureus* from growing in size. It is presumed that the nature of the cell wall explains curcumin's greater efficacy against Gram-positive (+) bacteria as opposed to Gram-negative (−) bacteria. Peptidoglycan and hydrophobic compounds make up the majority of gram-positive bacteria's cell walls, which facilitate easier penetration. On the other hand, the complicated composition of the outer membrane of Gram-negative bacteria acts as a barrier, preventing the entry of most hydrophobic compounds and antimicrobial drugs such as colistin, quinolones, and β-lactams (Górski et al., 2022). Being a hydrophobic molecule, gram-negative bacterial cell walls do not allow the penetration of the active curcumin inside the microbial cell.

Chitosan showed antibacterial activity against *E. coli*, *Pseudomonas aeruginosa*, and Klebsiella pneumoniae, as shown in Fig. 8 (b). At lower concentrations, it binds to the negatively charged surface of cells, particularly Gram-negative bacteria, disrupting cell membrane permeability and causing cell death by externalizing intracellular components. Conversely, higher concentrations of positively charged chitosan, attributed to amino groups, can coat the cell surface, trapping intracellular components inside the cell of microorganisms (Hosseinnejad & Jafari, 2016; Lim & Hudson, 2004). Moreover, in the case of Gram-positive bacteria, the positive charges on both bacterial cells and chitosan create a repelling effect, preventing their close interaction (Hosseinnejad & Jafari, 2016). Gram-negative bacteria are thought to respond to chitosan more than Gram-positive bacteria because of their hydrophilic nature. Chung et al. (Chung et al., 2004); Kong et al. (Kong et al., 2010), and Pavinatto et al. (Pavinatto et al., 2014) indicate a stronger bactericidal effect on Gram-negative bacteria, attributed to the

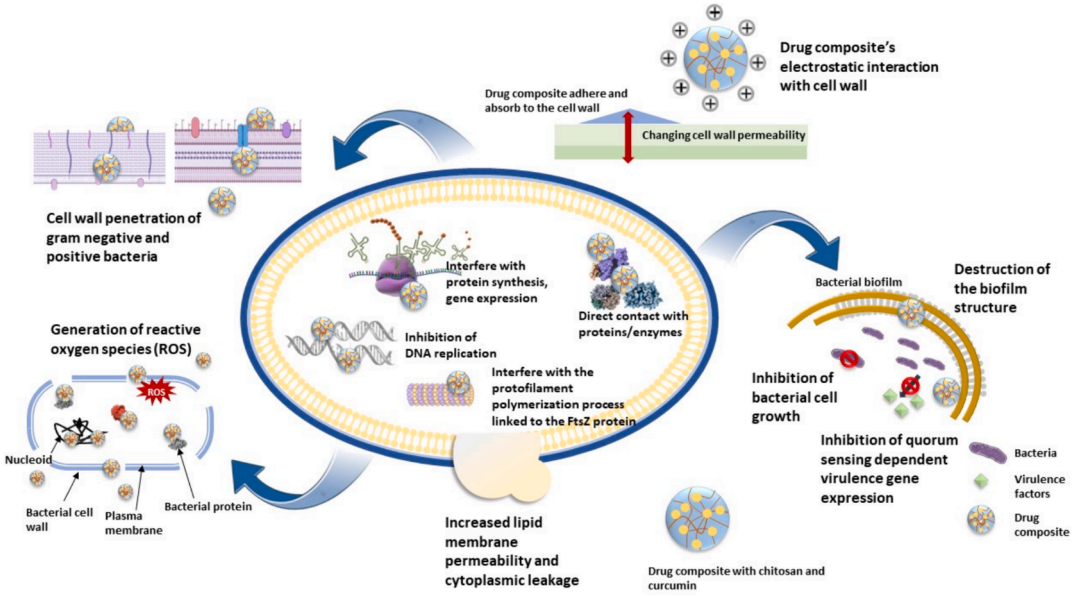

Fig. 10. Antibacterial mechanism of drug composite.

Table 4
MIC and MBC results of curcumin (cur), chitosan (chi) and composite.

Bacterial Strains	MIC (mg/ml)			MBC (mg/ml)			MBC/MIC		
	Cur:	**Chi:**	**Com:**	**Cur:**	**Chi:**	**Com:**	**Cur:**	**Chi:**	**Com:**
Pseudomonas aeruginosa	0.625	1.25	0.625	10	10	10	16	8	16
Staphylococcus aureus	0.625	1.25	0.625	10	5	10	16	4	16
Klebsiella pneumoniae	0.625	1.25	0.625	2.5	10	5	4	8	8
Escherichia coli	–	1.25	–	–	10	–	–	8	–

higher affinity between chitosan's amino groups and anionic radicals in the cell wall. Conversely, Hassan et al.(Hassan et al., 2018) and Helander et al.(Helander et al., 2001) suggest that Gram-positive bacteria may be more susceptible due to the presence of the gram-negative outer membrane barrier. The antimicrobial action involves chitosan being absorbed onto bacterial cell surfaces, causing increased lipid membrane permeability and the release of essential compounds, ultimately leading to cell death (Hosseinnejad & Jafari, 2016). Table 5 shows a summary of the relevant studies compared to the current study.

4. Conclusions

In the current study, an effective drug delivery system for curcumin was developed using chitosan as the biopolymer to improve curcumin's pharmacokinetics properties. Antioxidant, anti-inflammatory, and antibacterial activities of the developed composite material were tested simultaneously. According to the egg albumin denaturation assay and DPPH assay, the anti-inflammatory activity of the synthesized composite material varied from 25.36 % (0.2 mg/mL) to 68.84 % (1.6 mg/mL), while the antioxidant activity varied from 26.57 % (0.01 mg/mL) to 88.78 % (0.07 mg/mL), respectively. Drug composite had better antibacterial activity against the gram-positive *Staphylococcus aureus* strain as the easier penetration of the gram-positive cell wall structure. According to the results of the drug delivery study, curcumin was proven to have a sustained release over time based on Fickian diffusion and polymer relaxation (case II) transport mechanisms, which was proven by the n and m model parameters on KP and PS models, respectively. As per the values obtained, n values less than 0.43 correspond to the Fickian diffusion mechanism in polydispersed polymer matrices. Further, the differences in K_D and K_R constants in the PS model suggest that drug release from the polymer material does not solely depend on the Fickian diffusion, but the polymer relaxation also plays a significant role in releasing the curcumin from chitosan biopolymer. The limitations of the present study are the lack of in vivo experiments, the low water solubility of the delivery system due to the high molecular weight of chitosan, cytotoxicity assays, metabolic and excretion assays, and cumulative effects that may affect the drug safety. Hence, more in vivo assays for antioxidant and anti-inflammatory properties and drug delivery studies ought to be carried out. Furthermore, the ability to use chitosan as a carrier molecule to efficiently deliver curcumin to the target tissues should be assessed carefully through further research focusing on the possible effect of cytotoxicity and safety of the synthesized novel drug composite.

Funding

The authors thank the Sri Lanka Institute of Information Technology for funding this project.

CRediT authorship contribution statement

Supuni Wijayawardana: Writing – original draft, Methodology, Investigation, Formal analysis, Data curation, Conceptualization. **Charitha Thambiliyagodage:** Writing – review & editing, Supervision, Resources, Project administration, Methodology, Funding acquisition, Data curation, Conceptualization. **Madara Jayanetti:** Writing – review

Table 5
A comparison of the relevant studies reported in the literature with the current study.

Delivery system developed	Application	Reference
Forms of chitosan (beads, films, microspheres, nanoparticles, nanofibers, hydrogels, nanocomposites)	Chitosan and chitosan nanoparticles in drug delivery and their biocompatibility, low toxicity, and biodegradability	(Ali & Ahmed, 2018)
(PLGA) nanoparticles (NPs) loaded with curcumin modified with a glycopeptide (g7)	Brain delivery of curcumin and ability to influence Aβ pathology *in vitro*	(Barbara et al., 2017)
Chitosan-based drug nanoparticles (CSNPs) systems	Relationship between the modification in CSNPs as multifunctional delivery systems and drug release properties and kinetics of the drug release model	(Herdiana et al., 2022)
Curcumin-loaded chitosan nanoparticles	Chitosan facilitates the delivery of curcumin and improves the therapeutic effects on many chronic diseases, including cancer, bacterial infection, wound healing, Alzheimer's diseases, inflammatorybowel disease, and hepatitis C virus	(Hu & Luo, 2021)
Chitosan-based drug delivery systems	Preparation techniques of micro and nanoparticles of chitosan and applications in organ-targeting drug delivery	(Saikia & Gogoi, 2015)
Drug delivery systems for curcumin	Biomedical applications of using liposomes, nanoparticles loaded with PBCA, PLGA, and chitosan, polymer micelles, nanogels, nanocrystal suspension, nanoemulsion and self-microemulsion, and dendrimers and dimers.	(Sun et al., 2012)
Lotus root amylopectin (LRA)-chitosan (CS) composite hydrogen	Improve the solubility and stability of curcumin and enable it to be stable in the stomach and released in the small intestine.	(K. Liu et al., 2020)
Nanoliposomes and chitosan-coated nanoliposomes encapsulating curcumin	Enhanced the stability of nanoliposomes stability by chitosan coating and slowed the release of curcumin in the simulated gastrointestinal (GI) environment.	(Hasan et al., 2019)
Chitosan coated curcumin liposome	Temperature-dependent structure stability and sustained release of curcumin.	(Y. Liu et al., 2015)
Chitosan- PVP-based hydrogels	Biocompatible and biodegradable chitosan-based crosslinked hydrogel for *in vitro* release of encapsulated povidone-iodine	(Gull et al., 2020a)
Vinyltrimethoxy silane (VTMS) cross-linked chitosan/PVP hydrogels.	*In vitro* drug releasestudy for the controlled release of cephradine.	(Gull et al., 2019)
Epichlorohydrin cross-linked chitosan PVPhydrogel films	Inflammation targeted *in vitro* drug releasestudy for the controlled release of diclofenac sodium.	(Gull et al., 2020b)
Curcumin grafted chitosan drug delivery system.	Enhanced bioavailability and biocompatibility for sustained release of curcumin.	Current study

& editing, Supervision, Methodology, Data curation.

Appendix A. Supplementary material

Supplementary data to this article can be found online at https://doi.org/10.1016/j.arabjc.2024.105896.

References

Abadi, A.J., Mirzaei, S., Mahabady, M.K., Hashemi, F., Zabolian, A., Hashemi, F., Raee, P., Aghamiri, S., Ashrafizadeh, M., Aref, A.R., Hamblin, M.R., Hushmandi, K., Zarrabi, A., Sethi, G., 2022. Curcumin and its derivatives in cancer therapy: potentiating antitumor activity of cisplatin and reducing side effects. Phytother. Res. 36 (1), 189–213. https://doi.org/10.1002/PTR.7305.

Abdul Hameed, M.M., Mohamed Khan, S.A.P., Thamer, B.M., Al-Enizi, A., Aldalbahi, A., El-Hamshary, H., El-Newehy, M.H., 2020. Core-shell nanofibers from poly(vinyl alcohol) based biopolymers using emulsion electrospinning as drug delivery system for cephalexin drug. J. Macromol. Sci. Part A Pure Appl. Chem. 58 (2), 130–144. https://doi.org/10.1080/10601325.2020.1832517.

Adamczak, A., Ożarowski, M., Karpiński, T.M., 2020. Curcumin is a natural antimicrobial agent with strain-specific activity. Pharmaceuticals 13 (7), 1–12. https://doi.org/10.3390/ph13070153.

Ahmad, A., Mubharak, N.M., Naseem, K., Tabassum, H., Rizwan, M., Najda, A., Kashif, M., Bin-Jumah, M., Hussain, A., Shaheen, A., Abdel-Daim, M.M., Ali, S., Hussain, S., 2020. Recent advancement and development of chitin and chitosan-based nanocomposite for drug delivery: critical approach to clinical research. Arab. J. Chem. 13 (12), 8935–8964. https://doi.org/10.1016/j.arabjc.2020.10.019.

Ahmed, T., & Gilani, A. H. (2014). Therapeutic potential of turmeric in Alzheimer's disease: Curcumin or curcuminoids? In *Phytotherapy Research* (Vol. 28, Issue 4, pp. 517–525). John Wiley and Sons Ltd. doi: 10.1002/ptr.5030.

Ak, T., Gülçin, I., 2008. Antioxidant and radical scavenging properties of curcumin. Chem. Biol. Interact. 174 (1), 27–37. https://doi.org/10.1016/J.CBI.2008.05.003.

Al-Abdallah, B., Al-Faiyz, Y.S., Shaaban, S., 2022a. Anticancer, antimicrobial, and antioxidant activities of organodiselenide-tethered methyl anthranilates. Biomolecules 12 (12), 1765. https://doi.org/10.3390/BIOM12121765/S1.

Al-Abdallah, B., Al-Faiyz, Y.S., Shaaban, S., 2022b. Organoselenocyanates tethered methyl anthranilate hybrids with promising anticancer, antimicrobial, and antioxidant activities. Inorganics 10 (12), 246. https://doi.org/10.3390/INORGANICS10120246/S1.

Ali, A., Ahmed, S., 2018. A review on chitosan and its nanocomposites in drug delivery. Int. J. Biol. Macromol. 109, 273–286. https://doi.org/10.1016/J.IJBIOMAC.2017.12.078.

Anand, P., Kunnumakkara, A.B., Newman, R.A., Aggarwal, B.B., 2007. Bioavailability of curcumin: problems and promises. Mol. Pharm. 4 (6), 807–818. https://doi.org/10.1021/MP700113R/ASSET/IMAGES/MEDIUM/MP-2007-00113R_0003.GIF.

Andrews, J.M., 2001. Determination of minimum inhibitory concentrations. J. Antimicrob. Chemother. 48 (suppl_1), 5–16. https://doi.org/10.1093/JAC/48.SUPPL_1.5.

Anraku, M., Kabashima, M., Namura, H., Maruyama, T., Otagiri, M., Gebicki, J.M., Furutani, N., Tomida, H., 2008. Antioxidant protection of human serum albumin by chitosan. Int. J. Biol. Macromol. 43 (2), 159–164. https://doi.org/10.1016/J.IJBIOMAC.2008.04.006.

Azucena, R. C. I., Roberto, C. L. J., Martin, Z. R., Rafael, C. Z., Leonardo, H. H., Gabriela, T. P., & Araceli, C. R. (2019). Drug Susceptibility Testing and Synergistic Antibacterial Activity of Curcumin with Antibiotics against Enterotoxigenic Escherichia coli. *Antibiotics 2019, Vol. 8, Page 43*, *8*(2), 43. doi: 10.3390/ANTIBIOTICS8020043.

Bagheri, H., Ghasemi, F., Barreto, G.E., Rafiee, R., Sathyapalan, T., Sahebkar, A., 2020. Effects of curcumin on mitochondria in neurodegenerative diseases. BioFactors 46 (1), 5–20. https://doi.org/10.1002/biof.1566.

Balouiri, M., Sadiki, M., Ibnsouda, S.K., 2016. Methods for in vitro evaluating antimicrobial activity: a review. J. Pharm. Anal. 6 (2), 71–79. https://doi.org/10.1016/J.JPHA.2015.11.005.

Banerjee, S., Biswas, S., Chanda, A., Das, A., Adhikari, A., 2014. Evaluation of phytochemical screening and anti inflammatory activity of leaves and stem of Mikania scandens (l.) wild. Ann. Med. Health Sci. Res. 4 (4), 532. https://doi.org/10.4103/2141-9248.139302.

Barbara, R., Belletti, D., Pederzoli, F., Masoni, M., Keller, J., Ballestrazzi, A., Vandelli, M. A., Tosi, G., Grabrucker, A.M., 2017. Novel Curcumin loaded nanoparticles engineered for Blood-Brain Barrier crossing and able to disrupt Abeta aggregates. Int. J. Pharm. 526 (1–2), 413–424. https://doi.org/10.1016/j.ijpharm.2017.05.015.

Chandrasekaran, M., Kim, K.D., Chun, S.C., 2020. Antibacterial activity of chitosan nanoparticles: a review. Processes 8 (9), 1173. https://doi.org/10.3390/PR8091173.

Choukaife, H., Seyam, S., Alallam, B., Doolaanea, A.A., Alfatama, M., 2022. Current advances in chitosan nanoparticles based oral drug delivery for colorectal cancer treatment. Int. J. Nanomed. 17, 3933–3966. https://doi.org/10.2147/IJN.S375229.

Chung, Y.C., Su, Y.P., Chen, C.C., Jia, G., Wang, H.L., Wu, J.G., Lin, J.G., 2004. Relationship between antibacterial activity of chitosan and surface characteristics of cell wall. Acta Pharmacol. Sin. 25 (7), 932–936 http://www.chinaphar.com.

Cianciulli, A., Calvello, R., Ruggiero, M., Panaro, M.A., 2022. Inflammaging and brain: curcumin and its beneficial potential as regulator of microglia activation. Molecules 27 (2), 341. https://doi.org/10.3390/MOLECULES27020341.

Dei Cas, M., Ghidoni, R., 2019. Dietary curcumin: correlation between bioavailability and health potential. Nutrients 11 (9), 2147. https://doi.org/10.3390/nu11092147. MDPI AG.

Den Hartogh, D.J., Gabriel, A., Tsiani, E., 2019. Antidiabetic properties of curcumin II: evidence from in vivo studies. Nutrients 12 (1), 58. https://doi.org/10.3390/NU12010058.

Den Hartogh, D.J., Gabriel, A., Tsiani, E., 2020. Antidiabetic properties of curcumin I: evidence from in vitro studies. Nutrients 12 (1), 118. https://doi.org/10.3390/NU12010118.

Dutta, A.K., Ikiki, E., 2014. Novel drug delivery systems to improve bioavailability of curcumin. J. Bioequivalence Bioavailability 6 (1), 1–9. https://doi.org/10.4172/jbb.1000172.

Elisha, I.L., Dzoyem, J.P., McGaw, L.J., Botha, F.S., Eloff, J.N., 2016. The anti-arthritic, anti-inflammatory, antioxidant activity and relationships with total phenolics and total flavonoids of nine South African plants used traditionally to treat arthritis. BMC Complement. Altern. Med. 16 (1), 1–10. https://doi.org/10.1186/s12906-016-1301-z.

Eltaweil, A.S., Ahmed, M.S., El-Subruiti, G.M., Khalifa, R.E., Omer, A.M., 2023. Efficient loading and delivery of ciprofloxacin by smart alginate/carboxylated graphene oxide/aminated chitosan composite microbeads: In vitro release and kinetic studies. Arab. J. Chem. 16 (4), 104533 https://doi.org/10.1016/J.ARABJC.2022.104533.

Farzaei, M.H., Zobeiri, M., Parvizi, F., El-Senduny, F.F., Marmouzi, I., Coy-Barrera, E., Naseri, R., Nabavi, S.M., Rahimi, R., Abdollahi, M., 2018. Curcumin in liver diseases: a systematic review of the cellular mechanisms of oxidative stress and clinical perspective. Nutrients 10 (7), 855. https://doi.org/10.3390/NU10070855.

Gonfa, Y.H., Tessema, F.B., Bachheti, A., Rai, N., Tadesse, M.G., Nasser Singab, A., Chaubey, K.K., Bachheti, R.K., 2023. Anti-inflammatory activity of phytochemicals from medicinal plants and their nanoparticles: a review. Curr. Res. Biotechnol. 6, 100152 https://doi.org/10.1016/J.CRBIOT.2023.100152.

Górski, M., Niedźwiadek, J., Magryś, A., 2022. Antibacterial activity of curcumin – a natural phenylpropanoid dimer from the rhizomes of Curcuma longa L. and its synergy with antibiotics. Ann. Agric. Environ. Med. 29 (3), 394–400. https://doi.org/10.26444/aaem/148393.

Gouda, M., Khalaf, M.M., Shaaban, S., El-Lateef, H.M.A., 2022. Fabrication of chitosan nanofibers containing some steroidal compounds as a drug delivery system. Polymers 14 (10), 2094. https://doi.org/10.3390/POLYM14102094/S1.

Gull, N., Khan, S.M., Butt, M.T.Z., Zia, S., Khalid, S., Islam, A., Sajid, I., Khan, R.U., King, M.W., 2019. Hybrid cross-linked hydrogels as a technology platform for in vitro release of cephradine. Polym. Adv. Technol. 30 (9), 2414–2424. https://doi.org/10.1002/pat.4688.

Gull, N., Khan, S.M., Butt, O.M., Islam, A., Shah, A., Jabeen, S., Khan, S.U., Khan, A., Khan, R.U., Butt, M.T.Z., 2020a. Inflammation targeted chitosan-based hydrogel for controlled release of diclofenac sodium. Int. J. Biol. Macromol. 162, 175–187. https://doi.org/10.1016/j.ijbiomac.2020.06.133.

Gull, N., Khan, S.M., Khalid, S., Zia, S., Islam, A., Sabir, A., Sultan, M., Hussain, F., Khan, R.U., Butt, M.T.Z., 2020b. Designing of biocompatible and biodegradable chitosan based crosslinked hydrogel for in vitro release of encapsulated povidone-iodine: a clinical translation. Int. J. Biol. Macromol. 164, 4370–4380. https://doi.org/10.1016/j.ijbiomac.2020.09.031.

Gunes, H., Gulen, D., Mutlu, R., Gumus, A., Tas, T., Topkaya, A.E., 2016. Antibacterial effects of curcumin: an in vitro minimum inhibitory concentration study. Toxicol. Ind. Health 32 (2). https://doi.org/10.1177/0748233713498458.

Hamaguchi, T., Ono, K., Yamada, M., 2010. Review: Curcumin and Alzheimer's Disease. CNS Neurosci. Ther. 16 (5), 285–297. https://doi.org/10.1111/J.1755-5949.2010.00147.X.

Hamama, W.S., El-Bana, G.G., Shaaban, S., Zoorob, H.H., 2018. Synthetic approach to some new annulated 1,2,4-triazine skeletons with antimicrobial and cytotoxic activities. J. Heterocycl. Chem. 55 (4), 971–982. https://doi.org/10.1002/jhet.3127.

Hasan, M., Elkhoury, K., Kahn, C.J.F., Arab-tehrany, E., Linder, M., 2019. Curcumin in simulated environments. Molecules 24, 1–14.

Hassan, M.A., Omer, A.M., Abbas, E., Baset, W.M.A., Tamer, T.M., 2018. Preparation, physicochemical characterization and antimicrobial activities of novel two phenolic chitosan Schiff base derivatives. Sci. Rep. 8 (1) https://doi.org/10.1038/s41598-018-29650-w.

Helander, I.M., Nurmiaho-Lassila, E.-L., Ahvenainen, R., Rhoades, J., Roller, S., 2001. Chitosan disrupts the barrier properties of the outer membrane of Gram-negative bacteria. In. Int. J. Food Microbiol. 71 www.elsevier.comrlocaterijfoodmicro.

Herdiana, Y., Wathoni, N., Shamsuddin, S., & Muchtaridi, M. (2022). Drug release study of the chitosan-based nanoparticles. In *Heliyon* (Vol. 8, Issue 1). Elsevier Ltd. doi: 10.1016/j.heliyon.2021.e08674.

Hosseinnejad, M., & Jafari, S. M. (2016). Evaluation of different factors affecting antimicrobial properties of chitosan. In *International Journal of Biological Macromolecules* (Vol. 85, pp. 467–475). Elsevier B.V. doi: 10.1016/j.ijbiomac.2016.01.022.

Hu, Q., & Luo, Y. (2021). Chitosan-based nanocarriers for encapsulation and delivery of curcumin: A review. In *International Journal of Biological Macromolecules* (Vol. 179, pp. 125–135). Elsevier B.V. doi: 10.1016/j.ijbiomac.2021.02.216.

Huang, S., Beevers, 2011. Pharmacological and clinical properties of curcumin. Botanics: Targets and Therapy 5. https://doi.org/10.2147/btat.s17244.

Jadidi, A., Davoodian, F., Salahinejad, E., 2020. Effect of poly lactic-co-glycolic acid encapsulation on drug delivery kinetics from vancomycin-impregnated Ca-Mg silicate scaffolds. Prog. Org. Coat. 149 https://doi.org/10.1016/j.porgcoat.2020.105970.

Jafari, M., Parastouei, K., Abbaszadeh, S., 2023. Development of curcumin-loaded nanoemulsion stabilized with texturized whey protein concentrate: characterization,

stability and in vitro digestibility. Food Sci. Nutr. https://doi.org/10.1002/fsn3.3860.
Jayakumar, R., Chennazhi, K.P., Muzzarelli, R.A.A., Tamura, H., Nair, S.V., Selvamurugan, N., 2010. Chitosan conjugated DNA nanoparticles in gene therapy. Carbohydr. Polym. 79 (1), 1–8. https://doi.org/10.1016/J.CARBPOL.2009.08.026.
Jayanetti, M., Thambiliyagodage, C., Liyanaarachchi, H., Ekanayake, G., Mendis, A., Usgodaarachchi, L., 2024. In vitro influence of PEG functionalized ZnO–CuO nanocomposites on bacterial growth. Sci. Rep. 14 (1) https://doi.org/10.1038/s41598-024-52014-6.
Jiang, S., Han, J., Li, T., Xin, Z., Ma, Z., Di, W., Hu, W., Gong, B., Di, S., Wang, D., Yang, Y., 2017. Curcumin as a potential protective compound against cardiac diseases. Pharmacol. Res. 119, 373–383. https://doi.org/10.1016/J.PHRS.2017.03.001.
Jovanovic, S.V., Steenken, S., Boone, C.W., Simic, M.G., 1999. H-atom transfer is a preferred antioxidant mechanism of curcumin. J. Am. Chem. Soc. 121 (41), 9677–9681. https://doi.org/10.1021/JA991446M.
Keihanian, F., Saeidinia, A., Bagheri, R.K., Johnston, T.P., Sahebkar, A., 2018. Curcumin, hemostasis, thrombosis, and coagulation. J. Cell. Physiol. 233 (6), 4497–4511. https://doi.org/10.1002/JCP.26249.
Khar, A., Ali, A.M., Pardhasaradhi, B.V.V., Begum, Z., Anjum, R., 1999. Antitumor activity of curcumin is mediated through the induction of apoptosis in AK-5 tumor cells. FEBS Lett. 445 (1), 165–168. https://doi.org/10.1016/S0014-5793(99)00114-3.
Kim, Y., Zharkinbekov, Z., Raziyeva, K., Tabyldiyeva, L., Berikova, K., Zhumagul, D., Temirkhanova, K., & Saparov, A. (2023). Chitosan-Based Biomaterials for Tissue Regeneration. *Pharmaceutics 2023, 15*(3), 807. doi: 10.3390/PHARMACEUTICS15030807.
Kong, M., Chen, X.G., Xing, K., Park, H.J., 2010. Antimicrobial properties of chitosan and mode of action: A state of the art review. Int. J. Food Microbiol. 144 (1), 51–63. https://doi.org/10.1016/j.ijfoodmicro.2010.09.012.
Kulkarni, S.K., Dhir, A., 2010. An overview of curcumin in neurological disorders. Indian J. Pharm. Sci. 72 (2), 149. https://doi.org/10.4103/0250-474X.65012.
Kwon, Y., 2014. Curcumin as a cancer chemotherapy sensitizing agent. J. Korean Soc. Appl. Biol. Chem. 57 (2), 273–280. https://doi.org/10.1007/S13765-014-4077-1/METRICS.
Lao, L.L., Peppas, N.A., Boey, F.Y.C., Venkatraman, S.S., 2011. Modeling of drug release from bulk-degrading polymers. Int. J. Pharm. 418 (1), 28–41. https://doi.org/10.1016/J.IJPHARM.2010.12.020.
Li, J., Zhuang, S., 2020. Antibacterial activity of chitosan and its derivatives and their interaction mechanism with bacteria: current state and perspectives. Eur. Polym. J. 138, 109984 https://doi.org/10.1016/J.EURPOLYMJ.2020.109984.
Liang, Y.J., Yang, I.H., Lin, Y.W., Lin, J.N., Wu, C.C., Chiang, C.Y., Lai, K.H., Lin, F.H., 2021. Curcumin-loaded hydrophobic surface-modified hydroxyapatite as an antioxidant for sarcopenia prevention. Antioxidants 10 (4), 616. https://doi.org/10.3390/ANTIOX10040616/S1.
Lim, S.H., Hudson, S.M., 2004. Synthesis and antimicrobial activity of a water-soluble chitosan derivative with a fiber-reactive group. Carbohydr. Res. 339 (2), 313–319. https://doi.org/10.1016/j.carres.2003.10.024.
Liu, W., Zhai, Y., Heng, X., Che, F. Y., Chen, W., Sun, D., & Zhai, G. (2016). Oral bioavailability of curcumin: problems and advancements. In *Journal of Drug Targeting* (Vol. 24, Issue 8, pp. 694–702). Taylor and Francis Ltd. doi: 10.3109/1061186X.2016.1157883.
Liu, K., Huang, R.L., Zha, X.Q., Li, Q.M., Pan, L.H., Luo, J.P., 2020. Encapsulation and sustained release of curcumin by a composite hydrogel of lotus root amylopectin and chitosan. Carbohydr. Polym. 232 (October 2019), 115810 https://doi.org/10.1016/j.carbpol.2019.115810.
Liu, Y., Liu, D., Zhu, L., Gan, Q., Le, X., 2015. Temperature-dependent structure stability and in vitro release of chitosan-coated curcumin liposome. In: Food Res. Int., 74. https://doi.org/10.1016/j.foodres.2015.04.024. Elsevier B.V.
Mantzorou, M., Pavlidou, E., Vasios, G., Tsagalioti, E., Giaginis, C., 2018. Effects of curcumin consumption on human chronic diseases: a narrative review of the most recent clinical data. Phytother. Res. 32 (6), 957–975. https://doi.org/10.1002/PTR.6037.
Marcos Luciano Bruschi, 2015. Strategies to modify the drug release from pharmaceutical systems. Strategies to Modify the Drug Release from Pharmaceutical Systems. http://www.sciencedirect.com:5070/book/9780081000922/strategies-to-modify-the-drug-release-from-pharmaceutical-systems.
Mendis, A., Thambiliyagodage, C., Ekanayake, G., Liyanaarachchi, H., Jayanetti, M., Vigneswaran, S., 2023. Fabrication of naturally derived chitosan and ilmenite sand-based TiO2/Fe2O3/Fe-N-doped graphitic carbon composite for photocatalytic degradation of methylene blue under sunlight. Molecules 28 (7). https://doi.org/10.3390/molecules28073154.
Metzler, M., Pfeiffer, E., Schulz, S.I., Dempe, J.S., 2013. Curcumin uptake and metabolism. Biofactors 39 (1), 14–20. https://doi.org/10.1002/BIOF.1042.
Mirzaei, H., Shakeri, A., Rashidi, B., Jalili, A., Banikazemi, Z., Sahebkar, A., 2017. Phytosomal curcumin: A review of pharmacokinetic, experimental and clinical studies. In: Biomedicine and Pharmacotherapy, 85. Elsevier Masson SAS, pp. 102–112. https://doi.org/10.1016/j.biopha.2016.11.098.
Mishra, S., & Palanivelu, K. (2008). The effect of curcumin (turmeric) on Alzheimer's disease: An overview. In *Ann Indian Acad Neurol* (Vol. 11).
Mohan, T., Ajdnik, U., Nagaraj, C., Lackner, F., Dobaj Štiglic, A., Palani, T., Amornkitbamrung, L., Gradišnik, L., Maver, U., Kargl, R., Stana Kleinschek, K., 2022. One-step fabrication of hollow spherical cellulose beads: application in pH-responsive therapeutic delivery. ACS Appl. Mater. Interfaces 14 (3), 3726–3739. https://doi.org/10.1021/acsami.1c19577.
Mohebbi, S., Nezhad, M.N., Zarrintaj, P., Jafari, S.H., Gholizadeh, S.S., Saeb, M.R., Mozafari, M., 2018. Chitosan in biomedical engineering: a critical review. Curr. Stem Cell Res. Ther. 14 (2), 93–116. https://doi.org/10.2174/1574888X13666180912142028.
Morin-Crini, N., Lichtfouse, E., Torri, G., & Crini, G. (2019). *Fundamentals and Applications of Chitosan* (pp. 49–123). doi: 10.1007/978-3-030-16538-3_2.
Naksuriya, O., Okonogi, S., 2015. Comparison and combination effects on antioxidant power of curcumin with gallic acid, ascorbic acid, and xanthone. Drug Discoveries & Therapeutics 9 (2), 136–141. https://doi.org/10.5582/ddt.2015.01013.
Panahi, Y., Khalili, N., Sahebi, E., Namazi, S., Reiner, Ž., Majeed, M., Sahebkar, A., 2017. Curcuminoids modify lipid profile in type 2 diabetes mellitus: a randomized controlled trial. Complement. Ther. Med. 33, 1–5. https://doi.org/10.1016/J.CTIM.2017.05.006.
Pandey, A., Chaturvedi, M., Mishra, S., Kumar, P., Somvanshi, P., Chaturvedi, R., 2017. Reductive Metabolites of Curcumin and Their Therapeutic Effects. https://doi.org/10.1016/j.heliyon.2020.e05469.
Pavinatto, A., Souza, A.L., Delezuk, J.A.M., Pavinatto, F.J., Campana-Filho, S.P., Oliveira, O.N., 2014. Interaction of O-acylated chitosans with biomembrane models: Probing the effects from hydrophobic interactions and hydrogen bonding. Colloids Surf. B Biointerfaces 114, 53–59. https://doi.org/10.1016/j.colsurfb.2013.09.034.
Peng, Y., Ao, M., Dong, B., Jiang, Y., Yu, L., Chen, Z., Hu, C., Xu, R., 2021. Anti-inflammatory effects of curcumin in the inflammatory diseases: Status, limitations and countermeasures. In: Drug Design, Development and Therapy, 15. Dove Medical Press Ltd., pp. 4503–4525. https://doi.org/10.2147/DDDT.S327378
Peng, S., Li, Z., Zou, L., Liu, W., Liu, C., McClements, D.J., 2018. Improving curcumin solubility and bioavailability by encapsulation in saponin-coated curcumin nanoparticles prepared using a simple pH-driven loading method. Food Funct. 9 (3), 1829–1839. https://doi.org/10.1039/C7FO01814B.
Peppas, N. A., & Narasimhan, B. (2014). Mathematical models in drug delivery: How modeling has shaped the way we design new drug delivery systems. In *Journal of Controlled Release* (Vol. 190, pp. 75–81). Elsevier B.V. doi: 10.1016/j.jconrel.2014.06.041.
Perrone, D., Ardito, F., Giannatempo, G., Dioguardi, M., Troiano, G., Lo Russo, L., De Lillo, A., Laino, L., Lo Muzio, L., 2015. Biological and therapeutic activities, and anticancer properties of curcumin (Review). Experimental and Therapeutic Medicine 10 (5), 1615–1623. https://doi.org/10.3892/etm.2015.2749.
Prabha, S., Sowndarya, J., Ram, P.J.V.S., Rubini, D., Hari, B.N.V., Aruni, W., Nithyanand, P., 2021. Chitosan-coated surgical sutures prevent adherence and biofilms of mixed microbial communities. Curr. Microbiol. 78 (2), 502–512. https://doi.org/10.1007/S00284-020-02306-7/METRICS.
Priyadarsini, K.I., Maity, D.K., Naik, G.H., Kumar, M.S., Unnikrishnan, M.K., Satav, J.G., Mohan, H., 2003. Role of phenolic O-H and methylene hydrogen on the free radical reactions and antioxidant activity of curcumin. Free Radic. Biol. Med. 35 (5), 475–484. https://doi.org/10.1016/S0891-5849(03)00325-3.
Quadrado, R.F.N., Fajardo, A.R., 2020. Microparticles based on carboxymethyl starch/chitosan polyelectrolyte complex as vehicles for drug delivery systems. Arab. J. Chem. 13 (1), 2183–2194. https://doi.org/10.1016/J.ARABJC.2018.04.004.
Ritger, P.L., Peppas, N.A., 1987. A simple equation for description of solute release II. Fickian and anomalous release from swellable devices. J. Control. Release 5 (1), 37–42. https://doi.org/10.1016/0168-3659(87)90035-6.
Rodrigues, S., Dionísio, M., López, C.R., Grenha, A., 2012. Biocompatibility of Chitosan Carriers with Application in Drug Delivery. J. Funct. Biomater. 3 (3), 615–641. https://doi.org/10.3390/jfb3030615.
Rostami, E., Kashanian, S., Azandaryani, A.H., 2014. Preparation of solid lipid nanoparticles as drug carriers for levothyroxine sodium with in vitro drug delivery kinetic characterization. Mol. Biol. Rep. 41 (5), 3521–3527. https://doi.org/10.1007/s11033-014-3216-4.
Saikia, C., Gogoi, P., 2015. Chitosan: a promising biopolymer in drug delivery applications. J. Mol. Genet. Med. s4 https://doi.org/10.4172/1747-0862.s4-006.
Sak, M., Al-Faiyz, Y.S., Elsawy, H., Shaaban, S., 2022. Novel organoselenium redox modulators with potential anticancer, antimicrobial, and antioxidant activities. Antioxidants 11 (7), 1231. https://doi.org/10.3390/ANTIOX11071231/S1.
Samrot, A.V., Burman, U., Philip, S.A., Shobana, N., Chandrasekaran, K., 2018. Synthesis of curcumin loaded polymeric nanoparticles from crab shell derived chitosan for drug delivery. Inf. Med. Unlocked 10, 159–182. https://doi.org/10.1016/j.imu.2017.12.010.
Sánchez-Machado, D. I., López-Cervantes, J., Correa-Murrieta, M. A., Sánchez-Duarte, R. G., Cruz-Flores, P., & la Mora-López, G. S. (2018). Chitosan. In *Nonvitamin and Nonmineral Nutritional Supplements* (pp. 485–493). Elsevier. doi: 10.1016/B978-0-12-812491-8.00064-3.
Santel, T., Pflug, G., Hemdan, N.Y.A., Schäfer, A., Hollenbach, M., Buchold, M., Hintersdorf, A., Linder, I., Otto, A., Bigl, M., Oerlecke, I., Hutschenreuter, A., Sack, U., Huse, K., Groth, M., Birkemeyer, C., Schellenberger, W., Gebhardt, R., Platzer, M., Birkenmeier, G., 2008. Curcumin inhibits glyoxalase 1—a possible link to its anti-inflammatory and anti-tumor activity. PLoS One 3 (10), e3508.
Shaaban, S., Zarrouk, A., Vervandier-Fasseur, D., Al-Faiyz, Y.S., El-Sawy, H., Althagafi, I., Andreoletti, P., Cherkaoui-Malki, M., 2021. Cytoprotective organoselenium compounds for oligodendrocytes. Arabian J. Chem. 14 (4) https://doi.org/10.1016/J.ARABJC.2021.103051.
Shaaban, S., Adam, M.S.S., El-Metwaly, N.M., 2022. Novel organoselenium-based N-mealanilic acid and its zinc (II) chelate: catalytic, anticancer, antimicrobial, antioxidant, and computational assessments. J. Mol. Liq. 363, 119907 https://doi.org/10.1016/J.MOLLIQ.2022.119907.
Shariatinia, Z., 2019. Pharmaceutical applications of chitosan. Adv. Colloid Interface Sci. 263, 131–194. https://doi.org/10.1016/j.cis.2018.11.008. Elsevier B.V.

Siepmann, J., Siepmann, F., 2008. Mathematical modeling of drug delivery. Int. J. Pharm. 364 (2), 328–343. https://doi.org/10.1016/j.ijpharm.2008.09.004.
Srivastava, R.M., Singh, S., Dubey, S.K., Misra, K., Khar, A., 2011. Immunomodulatory and therapeutic activity of curcumin. Int. Immunopharmacol. 11 (3), 331–341. https://doi.org/10.1016/J.INTIMP.2010.08.014.
Sun, M., Su, X., Ding, B., He, X., Liu, X., Yu, A., Lou, H., Zhai, G., 2012. Advances in nanotechnology-based delivery systems for curcumin. In *Nanomedicine* (vol. 7 (7), 1085–1100. https://doi.org/10.2217/nnm.12.80.
Thambiliyagodage, C., Jayanetti, M., Mendis, A., Ekanayake, G., Liyanaarachchi, H., Vigneswaran, S., 2023. Recent advances in chitosan-based applications—a review. Materials 16 (5). https://doi.org/10.3390/ma16052073. MDPI.
Thandapani, G., Supriya Prasad, P., Sudha, P.N., Sukumaran, A., 2017. Size optimization and in vitro biocompatibility studies of chitosan nanoparticles. Int. J. Biol. Macromol. 104, 1794–1806. https://doi.org/10.1016/J.IJBIOMAC.2017.08.057.
Tomida, H., Fujii, T., Furutani, N., Michihara, A., Yasufuku, T., Akasaki, K., Maruyama, T., Otagiri, M., Gebicki, J.M., Anraku, M., 2009. Antioxidant properties of some different molecular weight chitosans. Carbohydr. Res. 344 (13), 1690–1696. https://doi.org/10.1016/J.CARRES.2009.05.006.
Truong, D.H., Nguyen, D.H., Ta, N.T.A., Bui, A.V., Do, T.H., Nguyen, H.C., 2019. Evaluation of the use of different solvents for phytochemical constituents, antioxidants, and in vitro anti-inflammatory activities of severinia buxifolia. J. Food Qual. 2019 https://doi.org/10.1155/2019/8178294.
Unagolla, J.M., Jayasuriya, A.C., 2018. Drug transport mechanisms and in vitro release kinetics of vancomycin encapsulated chitosan-alginate polyelectrolyte microparticles as a controlled drug delivery system. Eur. J. Pharm. Sci. 114, 199–209. https://doi.org/10.1016/j.ejps.2017.12.012.
Van Nong, H., Hung, L.X., Thang, P.N., Chinh, V.D., Vu, L.V., Dung, P.T., Van Trung, T., Nga, P.T., 2016. Fabrication and vibration characterization of curcumin extracted from turmeric (Curcuma longa) rhizomes of the northern Vietnam. Springerplus 5 (1). https://doi.org/10.1186/s40064-016-2812-2.
Varukattu, N.B., Vivek, R., Rejeeth, C., Thangam, R., Ponraj, T., Sharma, A., Kannan, S., 2020. Nanostructured pH-responsive biocompatible chitosan coated copper oxide nanoparticles: a polymeric smart intracellular delivery system for doxorubicin in breast cancer cells. Arab. J. Chem. 13 (1), 2276–2286. https://doi.org/10.1016/J.ARABJC.2018.04.012.
Venkatesan, N., Punithavathi, D., Babu, M., 2007. Protection from acute and chronic lung diseases by curcumin. Adv. Exp. Med. Bio. 595, 379–405. https://doi.org/10.1007/978-0-387-46401-5_17/COVER.
Verlee, A., Mincke, S., Stevens, C.V., 2017. Recent developments in antibacterial and antifungal chitosan and its derivatives. Carbohydr. Polym. 164, 268–283. https://doi.org/10.1016/J.CARBPOL.2017.02.001.
Wechsler, M. E., Vela Ramirez, J. E., & Peppas, N. A. (2019). 110th Anniversary: Nanoparticle Mediated Drug Delivery for the Treatment of Alzheimer's Disease: Crossing the Blood-Brain Barrier. In *Industrial and Engineering Chemistry Research* (Vol. 58, Issue 33, pp. 15079–15087). American Chemical Society. doi: 10.1021/acs.iecr.9b02196.
Wójcik-Pastuszka, D., Krzak, J., Macikowski, B., Berkowski, R., Osiński, B., Musiał, W., 2019. Evaluation of the release kinetics of a pharmacologically active substance from model intra-articular implants replacing the cruciate ligaments of the knee. Materials 12 (8). https://doi.org/10.3390/ma12081202.
Wongcharoen, W., Phrommintikul, A., 2009. The protective role of curcumin in cardiovascular diseases. Int. J. Cardiol. 133 (2), 145–151. https://doi.org/10.1016/j.ijcard.2009.01.073.
Xie, L., Li, X.K., Takahara, S., 2011. Curcumin has bright prospects for the treatment of multiple sclerosis. Int. Immunopharmacol. 11 (3), 323–330. https://doi.org/10.1016/J.INTIMP.2010.08.013.
Yavarpour-Bali, H., Pirzadeh, M., Ghasemi-Kasman, M., 2019. Curcumin-loaded nanoparticles: a novel therapeutic strategy in treatment of central nervous system disorders. Int. J. Nanomed. 14, 4449–4460. https://doi.org/10.2147/IJN.S208332.
Yesmin, S., Paul, A., Naz, T., Rahman, A.B.M.A., Akhter, S.F., Wahed, M.I.I., Emran, T.B., Siddiqui, S.A., 2020. Membrane stabilization as a mechanism of the anti-inflammatory activity of ethanolic root extract of Choi (Piper chaba). Clin. Phytosci. 6 (1) https://doi.org/10.1186/s40816-020-00207-7.
Yixuan, L., Qaria, M. A., Sivasamy, S., Jianzhong, S., & Daochen, Z. (2021). Curcumin production and bioavailability: A comprehensive review of curcumin extraction, synthesis, biotransformation and delivery systems. In *Industrial Crops and Products* (Vol. 172). doi: 10.1016/j.indcrop.2021.114050.
Yu, Y., Shen, Q., Lai, Y., Park, S.Y., Ou, X., Lin, D., Jin, M., Zhang, W., 2018. Anti-inflammatory effects of curcumin in microglial cells. Front. Pharmacol. 9 (APR), 345045 https://doi.org/10.3389/FPHAR.2018.00386/BIBTEX.
Yun, D.G., Lee, D.G., 2016. Antibacterial activity of curcumin via apoptosis-like response in Escherichia coli. Appl. Microbiol. Biotechnol. 100 (12), 5505–5514. https://doi.org/10.1007/s00253-016-7415-x.
Zheng, D., Huang, C., Huang, H., Zhao, Y., Khan, M. R. U., Zhao, H., & Huang, L. (2020). Antibacterial Mechanism of Curcumin: A Review. In *Chemistry and Biodiversity* (Vol. 17, Issue 8). Wiley-VCH Verlag. doi: 10.1002/cbdv.202000171.